Intracellular Signal-Responsive Gene Carrier for Cell-Specific Gene Expression

Kenji Kawamura,† Jun Oishi,† Jeong-Hun Kang,‡ Kota Kodama,‡ Tatsuhiko Sonoda,† Masaharu Murata,† Takuro Niidome,† and Yoshiki Katayama*,†,‡

Department of Applied Chemistry, Faculty of Engineering, Kyushu University, Hakozaki, Higashi-ku, Fukuoka 812-8581, and CREST, Japan Science and Technology Agency, 4-1-8 Honcho, Kawaguchi-shi, Saitama 332-0012, Japan

Received September 28, 2004; Revised Manuscript Received November 6, 2004

We designed a peptide−polymer conjugate (CPCCtat) as a novel gene carrier that could control gene expression responding to the intracellular caspase-3 signal. This carrier consists of an uncharged main polymer chain and a cationic peptide side chain, which includes the substrate sequence of caspase-3 and the protein transduction domain sequence of HIV-1 Tat. In the present study, CPCCtat formed a tight complex with DNA through an electrostatic interaction, and in this state the gene expression was totally suppressed. In contrast, the complex disintegrated in the presence of caspase-3 due to cleavage of the cationic portion from CPCCtat. This event led to an activation of gene expression. Our results also indicate that the complex can be delivered into living cells due to the cell-permeable peptide side chain of CPCCtat. This intracellular signal-responsive system with CPCCtat will be useful for the cell-specific gene expression system.

Introduction

Recent progress in genomic research has revealed novel genes related to various diseases and has made it possible to apply them to gene therapies. In fact, 918 protocols have already been carried out in clinical trials.[1] To further generalize gene therapy, however, it is necessary for expression of the delivered gene to be activated only in the target cell to avoid side effects. In fact, some serious side effects in gene therapy have been reported due to nonspecific gene expression in untargeted cells. Thus, many targeting strategies have been investigated in various drug and gene delivery systems.[2−7] These strategies often utilize the interaction between a molecular marker on the cellular surface that is specific to the target disease cells and the ligand molecules attached to the gene carrier. However, this so-called active targeting strategy is sometimes not very successful because the effective molecular markers are not always available. Therefore, the present applications of gene therapy have been restricted to cases that do not require control of the delivered gene expression.

We propose herein a novel strategy that can discriminate normal cells and target cells in gene therapy by focusing on differences in intracellular signals. Living cells possess elaborate molecular reaction cascades, referred to as an intracellular signal transduction system, in individual cells to regulate cellular functions and responses. Hyperactivation of certain intracellular signals is often seen in many diseases.[8−15] Thus, if such unusual intracellular signals could be used to activate the delivered gene, cell-selective control of the delivered gene expression could be achieved. We have previously reported a drug capsule and gene carrier system that releases drug activity or gene expression, respectively, responding to a certain intracellular kinase or protease signal.[16−18] However, the gene carrier reported previously could not deliver DNA into living cells, although these materials worked well in cell-free systems.

In the present study, we designed a novel cell-permeable gene carrier that can activate the delivered gene in response to the intracellular caspase-3 signal, which is a cysteinyl protease and plays an important role in apoptosis. Control of gene expression depending on the activation of intracellular caspase-3 was demonstrated using a cellular sample. We term this approach for gene delivery with cell-signal-specific gene expression D-RECS (drug delivery system responding to cellular signaling).

Materials and Methods

Preparation of the Caspase-3-Responsible Polymer CPCCtat. CPCCtat was synthesized in a manner similar to that described previously.[16,17] Thus, a methacryloyl peptide (6.6 mg, 2.67 μmol) in which the methacryloyl group was attached at the amino terminus of the peptide and the acrylamide (10 mg, 140 μmol) were dissolved in degassed water and allowed to stand at room temperature for 1 h after the addition of ammonium persulfate (1.1 mg, 4.82 μmol) and *N,N,N′,N′*-tetramethylethylenediamine (1.42 μL, 9.48 μmol) as the redox initiator couple. The product was then purified by overnight dialysis against water using a semipermeable membrane bag (with a molecular weight cutoff of 25000), followed by lyophilization to obtain a white powder at 30% yield.

* To whom correspondence should be addressed. E-mail: ykatatcm@mbox.nc.Kyushu-u.ac.jp.
† Kyushu University.
‡ Japan Science and Technology Agency.

10.1021/bm0493887 CCC: $30.25
Published on Web 00/00/0000 PAGE EST: 5.1

Gel Electrophoresis. Linear DNA (1234 bp, 0.1 μg) which was a restriction fragment from pRL-null was dissolved in 2 μL of sterile water. The CPCCtat was then added to the solution at various concentrations. All solutions were diluted to 4.2 μL with sterile water, allowed to stand for 15 min at room temperature, and then analyzed by 1% agarose gel electrophoresis in Tris−borate buffer (pH 8.0). For the caspase-3 reaction, activated caspase-3 (2 U, CHEMICON) was added to each solution, and the resulting solutions were incubated for 90 min at 37 °C before being subjected to gel electrophoresis.

Luciferase Expression in a Cell-Free System. All experiments were performed using a cell-free expression system (T7 S30 extract system for circular DNA, Promega) containing the T7 S30 extract and an amino acid mixture. Luciferase was expressed for 40 min at 37 °C using luciferase-encoding DNA (pRL-CMV). To prepare the CPCCtat−DNA 1:1 complex, the CPCCtat was mixed with the DNA (1 μg) at a concentration in which the ratio of the cationic charge of the CPCCtat (the net charge of each peptide side chain was assumed to be +5) to the phosphate residue in the DNA was 1.0, 15 min before the expression experiment. In the treatment of the 1:1 complex with caspase-3, the solution containing the DNA−CPCCtat complex was preincubated with activated caspase-3 (2 U) for 1.0 h at 37 °C, and 5 μg (10 nmol) of a caspase-3 inhibitor (Ac-DEVD-CHO) was then added before the expression experiment. In the experiment using factor Xa, factor Xa (1 μg) was used instead of caspase-3. In the control experiment, luciferase was expressed using the solution containing 1 μg of the DNA (4.8 nmol/μL as the phosphate residue) without CPCCtat or caspase-3. To monitor the chemiluminescence, 10 μL of the reaction mixture was added to the luciferase assay solution (Promega), and the chemiluminescence was measured using a multilabel counter, ARVO (WALLAC Inc.).

The determination of messenger RNA was performed using an RNA6000 Nano assay kit (Agilent Technologies) and Agilent 2100 bioanalyzer. Typically, an aliquot of the reaction mixture was loaded onto the gel microchip, in which a fluorescent probe for messenger RNA detection had been premixed, and the target messenger RNA was separated with electrophoresis. Then, the target messenger RNA was quantified by comparing its band area with that of marker RNA.

Delivery of the DNA−CPCCtat Complex into NIH 3T3 Cells and Regulation of Gene Expression by Intracellular Apoptotic Signals. NIH 3T3 cells (1×10^4 cells) were seeded into each well of a 96-well microtiter plate and incubated with Dulbecco's modified Eagle's medium (DMEM) supplemented with 10% fetal bovine serum (FBS) at 37 °C under a 5% CO_2 atmosphere. After an overnight incubation, the culture medium was exchanged to OPTI-MEM without serum. The EGFP-encoding DNA−CPCCtat complex at a charge ratio of 1.0 was delivered into the NIH 3T3 cells in the presence or absence of apoptotic stimulation. For the apoptotic stimulation, the cells were pretreated with staurosporin (50 μM). Delivery of the DNA−CPCCtat complex into the NIH 3T3 cells was as follows. pEGFP (0.1 μg) was incubated with the CPCCtat (0.92 mg) in 2 μL of sterile water for 15 min to form the complex. The complex solution was then diluted to 100 μL with OPTI-MEM and added to each well, followed by incubation for 2 h under a 5% CO_2 atmosphere at 37 °C.

Delivery of the CPCCtat−DNA Complex with HVJ-E (Envelope of Hemagglutinating Virus of Japan) and Regulation of Gene Expression Responding to Intracellular Apoptotic Signals. The DNA−CPCCtat complex was transfected into NIH 3T3 cells using GenomONE (HVJ-E) purchased from Ishihara Industries. NIH 3T3 cells (1×10^4 cells) were seeded into each well of a 96-well microtiter plate and incubated in DMEM with 10% FBS at 37 °C under a 5% CO_2 atmosphere. After an overnight incubation, the EGFP-encoding DNA−CPCCtat complex at a charge ratio of 1.0 or 2.0 encapsulated in HVJ-E was delivered into the NIH 3T3 cells. The DNA−CPCCtat complex was encapsulated into HVJ-E according to the protocol recommended by the supplier with slight modification.

In brief, one assay unit (20 μL) of HVJ-E was centrifuged at 10000 rpm for 5 min at 4 °C. After removal of the supernatant, the pellet was suspended in 5 μL of buffer solution. The suspension was mixed with 16 μL of EGFP-encoding DNA−CPCCtat complex solution (0.8 μg of DNA and CPCCtat at a charge ratio of 1.0) and 2.1 μL of reagent B (detergent). The mixture was centrifuged at 10000 rpm for 5 min at 4 °C. After removal of the supernatant, the pellet was suspended with 12.5 μL of buffer solution and then mixed with 5 μL of reagent C (protamine sulfate). Next, 2 μL of this mixture was diluted with OPTI-MEM (with 5% FBS) to 100 μL, and this suspension was added to a well in a 96-well plate. After a 1 h incubation, staurosporine was added to the cultured medium (final concentration 1 μM). The plate was incubated at 37 °C under a 5% CO_2 atmosphere for 15 h, and observed with a confocal laser scan microscope. Preparation of the DNA−CPCCtat complex was described above.

Results and Discussion

Design and Preparation of the Caspase-3-Responsible Polymer CPCCtat. To achieve cell-selective gene expression, we designed a novel polymer that could activate the delivered gene expression responding to the intracellular caspase-3 signal. The polymer CPCCtat (cationic polymer possessing the cleavage site for caspase-3) is a graft-type copolymer that is composed of polyacrylamide for the main chain and cationic peptide for the side chain (Figure 1a). This peptide side chain contains a consensus amino acid sequence, DEVD (anionic), for the selective cleavage site of caspase-3[19] and the protein transduction domain sequence of HIV-1 Tat protein (Tat peptide, GRKKRRQRRRPPQ) for the cationic portion and cell-permeable unit.[20,21] This polymer was obtained in good yield using methacryloyl peptide monomer and acrylamide with radical polymerization. The resulting CPCCtat contained the peptide side chain at a concentration of 0.81 mol % as the monomer unit content, estimated by the results of elemental analysis. CPCCtat forms a stable complex with DNA through an electrostatic interaction, and this complex is taken up by living cells due to the cell-permeable peptide in CPCCtat.

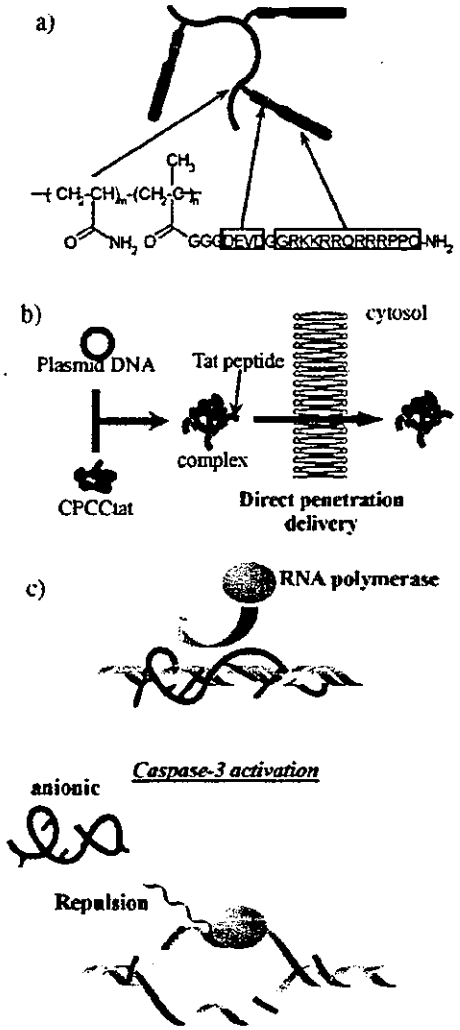

Figure 1. Concept of the gene delivery and gene regulation system with the intracellular caspase-3 signal-responsive polymer CPCCtat. (a) Structure of CPCCtat. CPCCtat consists of acrylamide as the main chain and peptides as the side chain. The pendant peptides include the anionic caspase-3 cleavage site (blue) and a cell-permeable cationic portion (red). (b) Cellular uptake of the CPCCtat–DNA complex. The CPCCtat forms stable complexes with DNA through electrostatic interactions. The protein transduction domain sequence (Tat peptide) of the side chain peptide in CPCCtat then leads the CPCCtat–DNA complex into the cell. (c) Mechanistic scheme of artificial gene regulation responding to caspase-3. When the CPCCtat forms a complex with the DNA, gene expression is suppressed. When the intracellular caspase-3 is activated, the cationic portion of the peptide in the CPCCtat is cleaved with caspase-3. These events cause a disintegration of the complex and release the DNA to activate gene transcription.

Figure 1c shows the concept of gene regulation with the CPCCtat–DNA complex. In the polymer–DNA complex, CPCCtat suppresses the accessibility of RNA polymerase to the DNA strand. In contrast, when the intracellular caspase-3 is continuously activated, this complex is disintegrated due to cleavage of the cationic portion of the peptide side chain from the main polymer chain. In this case, the net charge of the polymer changes from cationic to anionic, and free DNA is released from the polymer–DNA complex by an electrostatic repulsion between DNA and the residual polymer that is produced from CPCCtat with the caspase-3 cleavage reaction. As a result, caspase-3 signaling should accelerate gene expression.

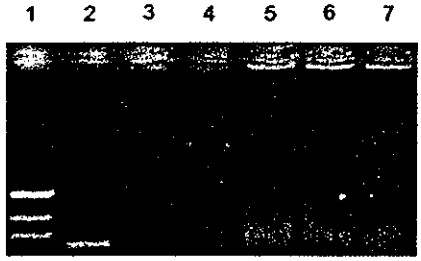

Figure 2. Formation of the CPCCtat–DNA complex and its disintegration with caspase-3 signaling. Lanes 2–4 and 5–7 show the electropherograms of the DNA–CPCCtat complex in the absence and presence of caspase-3, respectively. The ratio of the cationic charge of the CPCCtat (the net charge of each pendant peptide was assumed to be +5) to the phosphate residue in the DNA was 1.0 in lanes 3 and 6, and 2.0 in lanes 4 and 7. Lanes 2 and 5 did not contain the CPCCtat. Lane 1 shows the 1 kb DNA ladder.

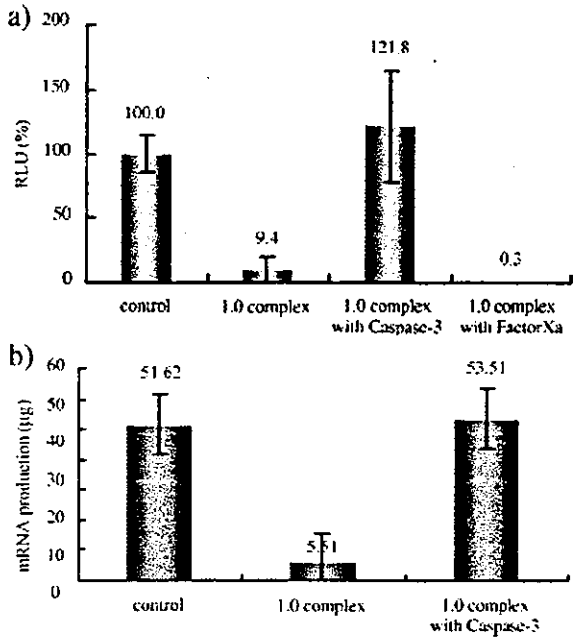

Figure 3. Suppression of luciferase expression with the CPCCtat and its cancellation with caspase-3 signaling in a cell-free system. (a) Luciferase expression in the presence of CPCCtat with or without active caspase-3. (b) Determination of the messenger RNA under the same conditions as in (a).

Effect of Caspase-3 on the Stability of the CPCCtat–DNA Complex and Regulation of Gene Expression in a Cell-Free System. We first investigated whether CPCCtat actually worked as a substrate for caspase-3 using MALDI-TOF mass spectrometry. When the peptide side chain on the CPCCtat is cleaved with caspase-3, the cationic segment of the peptide side chain should be cut off as a fragment peptide (GGRKKRRQRRRPPQ-NH_2, *m/e* = 1775.42). The fragment peptide was detected on the basis of the MS measurement, even in the CPCCtat–DNA complex (data not shown). These results suggest that caspase-3 recognizes the substrate sequence on the side chain in the presence of electrostatic interactions with DNA.

Therefore, the effects of the caspase-3 reaction on the stability of the DNA–CPCCtat complex were investigated using an agarose gel electrophoresis experiment. Addition of the CPCCtat polymer to the DNA solution suppressed the mobility of DNA, indicating the formation of the

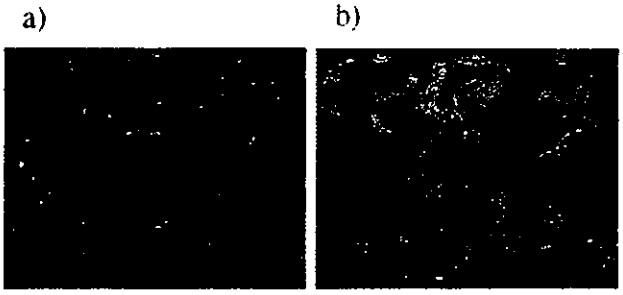

Figure 4. Delivery of the fluorescein-labeled DNA into the NIH 3T3 cell using CPCCtat. (a) Addition of fluorescein-labeled DNA to living cells. (b) Addition of the CPCCtat–fluorescein-labeled DNA complex to living cells.

CPCCtat–DNA complex (Figure 2, lanes 3 and 4). On the other hand, this effect completely disappeared in the presence of active caspase-3 (Figure 2, lanes 6 and 7). This result suggested that the caspase-3 signal could disintegrate the CPCCtat–DNA complex to release the free DNA. Similar polymer–DNA complex formation and disintegration with caspase-3 were observed by atomic force microscopy (data not shown). Figure 3a shows the regulation of gene expression by CPCCtat in a cell-free system. Luciferase expression was significantly suppressed in the formation of the CPCCtat–DNA complex. However, the addition of active caspase-3 to this complex returned the expression ratio to 100% compared with that of free DNA (control). In contrast, when we used another protease, factor Xa, gene expression did not recover. The messenger RNA levels were also determined in each experiment. The mRNA levels in the presence of CPCCtat or after treatment with caspase-3 corresponded to the gene expression levels under the same conditions (Figure 3b). These results indicate that CPCCtat can regulate gene expression in its transcription step on the basis of the change of the carrier–DNA complex stability, and that its activation is selective in response to the caspase-3 signal.

Gene Delivery Using CPCCtat and the Apoptotic Cell-Specific Gene Expression of the Delivered Gene in Cultured Cells. All the results mentioned above were very similar to those obtained in our previous research using a similar polymer–peptide conjugate (CPCC), which had oligolysine instead of a Tat peptide as the cationic portion. However, our previous polymer (CPCC) could not deliver any genes into living cells. Therefore, in the present study we applied the CPCCtat system to gene delivery into cells because CPCCtat possesses as its cationic region the Tat peptide, which is a cellular membrane-permeable peptide, a so-called PTD (protein transduction domain). In fact, the complex derived from CPCCtat and fluorescein-labeled DNA (1234 bp) at a charge ratio of 1 was successfully delivered into NIH 3T3 cells on the basis of fluorescence microscope observations (Figure 4). This improvement in transfection efficiency depends on the existence of the Tat peptide, which facilitates the internalization of the CPCCtat–DNA complex in a nonendocytotic manner. After the gene was delivered using CPCCtat, regulation of gene expression in response to intracellular caspase-3 was possible. When a GFP-encoding plasmid was delivered with the CPCCtat for 15 min at 37 °C, no fluorescence was observed in any cells after 24 h, meaning that gene expression was totally suppressed. In contrast, when a GFP-encoding plasmid was delivered into the caspase-3-activated cells, which was stimulated by staurosporine, weak fluorescence derived from GFP was observed in the cytosol after 4 h of delivery (data not shown). However, this fluorescence intensity was so weak that more sensitivity was necessary to evaluate the extent of gene expression quantitatively responding to the intracellular caspase-3 signaling, probably due to the poor efficiency of gene delivery into the cells. We therefore tried to increase the amount of CPCCtat–DNA complex incorporated into living cells using HVJ-E. HVJ-E is an inactivated virus envelope, and it can deliver a gene inside its

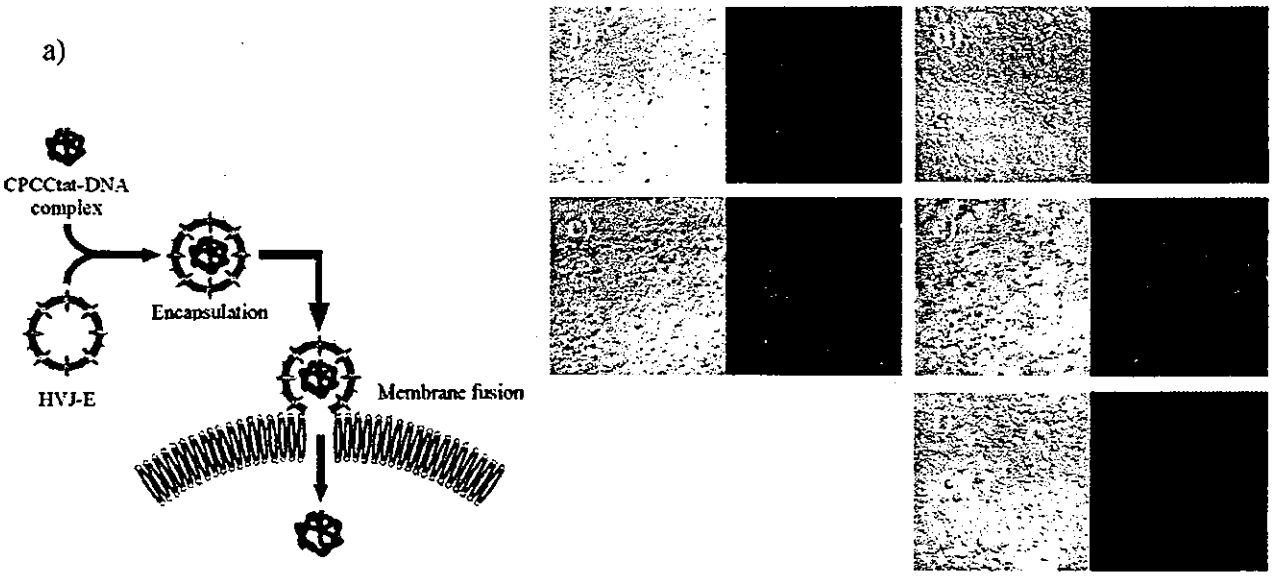

Figure 5. Delivery of the CPCCtat–DNA complex to NIH 3T3 cells with HVJ-E and apoptotic cell-selective expression of GFP. (a) Scheme of the CPCCtat–DNA complex delivery into cells with HVJ-E. (b–f) GFP-encoding DNA–CPCCtat complexes at a charge ratio of 1.0 and 2.0 were encapsulated by HVJ-E and delivered into NIH 3T3 cells without apoptotic stimulation (b and d), or 15 h after apoptotic stimulation (c and e). (f) Same experiment as (e) using $CPCC_{EVEE}$ instead of CPCCtat. One hour after the addition of the HVJ-E-encapsulating CPCCtat–DNA complex, the cells were treated with staurosporin as the apoptotic stimulant (c, e, f).

envelope through membrane fusion between HVJ-E and the target cell.[22] We applied HVJ-E to encapsulate the CPCCtat–DNA complex. The HVJ-E-encapsulating CPCCtat–DNA complex was taken up by the cultured cells through membrane fusion, and the polymer–DNA complex inside the HVJ-E was effectively delivered into the cells (Figure 5a). The CPCCtat–DNA (GFP-encoding) complex at a charge ratio of 1 or 2 (+/−) was successfully incorporated into HVJ-E. Then, the HVJ-E encapsulating the CPCCtat–DNA complex was added to the NIH 3T3 cells. When the complex at a charge ratio of 1 was delivered into the cells, weak fluorescence derived from GFP was observed after 16 h of delivery (Figure 5b), even in normal cells without apoptotic stimulation. On the other hand, the expression of GFP was completely suppressed in normal cells in the case of a charge ratio of 2 (Figure 5d). These results probably indicate that the increase in cationic polymer levels more effectively augments the steric hindrance of the acrylamide main chain in CPCCtat to prevent the access of RNA polymerase to DNA in the case of a charge ratio of 2. We monitored the fluorescence in the cellular sample for 2 days after addition of the complex, but any gene expression did not appear. This suppression of gene expression cannot be applied with similar efficiency to ordinary cationic polymers such as poly-L-lysine or its derivatives. In fact, poly-L-lysine cannot suppress luciferase expression under the same conditions as those shown in Figure 3a.

CPCCtat activated GFP expression only in the case of caspase-3 activation (Figure 5c,e). After 15 h of stimulation with staurosporine (1 μM), fluorescence derived from GFP was observed in complex-delivered cells with charge ratios of both 1 and 2. We estimated the intracellular activity of caspase-3 using a fluorescent substrate of caspase-3 (Ac-DEVD-NH-coumarin) by monitoring the fluorescence intensity at 490 nm (data not shown). In this case, the activity of the intracellular caspase-3 was around 2 U after 2–3 h of the staurosporine treatment. This activity was similar to that which we used in the cell-free experiment. Thus, it was reasonable that this activation of the gene expression was caused by the intracellular caspase-3. Additionally, we examined the same experiment with the control polymer $CPCC_{EVEE}$, in which the substrate sequence of DEVD was changed to EVEE. This sequence does not work as the substrate of caspase-3, but it has the same anionic charge as DEVD. Figure 5f shows the results of the GFP expression assay with $CPCC_{EVEE}$ using NIH 3T3 cells. Under these conditions, no fluorescence was observed, even if the caspase-3 was activated with staurosporine. These results indicate that CPCCtat can actually regulate the delivered gene expression in the living cells specifically responding to the intracellular caspase-3 signaling. We are now trying to rescue target cells from apoptosis, using the apoptosis inhibitor-encoding gene with the CPCCtat system.

Conclusion

We report here a new class of gene carrier based on the D-RECS system. The CPCCtat polymer can activate the delivered gene expression responding to target intracellular signaling (caspase-3 activity). This system should advance the development of cell-specific gene therapy, since the occurrence of unusual intracellular signaling is essential in almost all diseases. Our strategy therefore has the potential to be applied to various diseases. In fact, we have previously reported another type of polymer–peptide conjugate responding to protein kinase A signaling. This polymer regulates gene expression in a cell-free system very similarly to the CPCCtat polymer. Such systems will offer a new approach to the design of a cell-specific gene expression system.

Acknowledgment. This work was financially supported by CREST, the Japan Science Corp., a grant-in-aid for Scientific Research from the Ministry of Education, Science, Sports, and Culture in Japan, and a grant-in-aid for Scientific Research from the Ministry of Health, Labour and Welfare.

References and Notes

(1) http://www.wiley.co.uk/wileychi/genmed/clinical/.
(2) Varga, C. M.; Wickham, T. J.; Lauffenburger, D. A. Receptor-Mediated Targeting of Gene Dlivery Vectors: Insights from Molecular Mechanisms for Improved Vehicle Design. *Biotechnol. Bioeng.* 2000, *70*, 593–605.
(3) Hood, J. D.; Bednarski, M.; Frausto, R.; Guccione, S.; Reisfeld, R. A.; Xiang, R.; Cheresh, D. A. Tumor Regression by Targeted Gene Delivery to the Neovasculature. *Science* 2002, *296*, 2404–2407.
(4) Meers, P. Enzyme-activated targeting of liposomes. *Adv. Drug Delivery Rev.* 2001, *53*, 265–272.
(5) Torchilin, V. P. Drug targeting. *Eur. J. Pharm. Sci.* 2000, *11*, S81–S91.
(6) Garnett, M. C. Targeted drug conjugates: principles and progress. *Adv. Drug Delivery Rev.* 2001, *53*, 171–216.
(7) Kato, Y.; Onishi, H.; Machida, Y. Biological characteristics of lactosaminated N-succinyl-chitosan as a liver-specific drug carrier in mice. *J. Controlled Release* 2001, *70*, 295–307.
(8) Hartmann, A.; Hunot, S.; Michel, P. P.; Muriel, M. P.; Vyas, S.; Faucheux, B. A.; Mouatt-Prigent, A.; Turmel, H.; Srinivasa, A.; Ruberg, M.; Evan, G. I; Agid, Y.; Hirsch, E. C. Caspase-3: A vulnerability factor and final effector in apoptotic death of dopaminergic neurons in Parkinson's disease. *Proc. Natl. Acad. Sci. U.S.A.* 2000, *97*, 2875–2880.
(9) Gopalakrishna, R.; Jaken, S. Protein kinase C signaling and oxidative stress. *Free Radical Biol. Med.* 2000, *28*, 1349–1361.
(10) Graff, J. R.; Konicek, B. W.; McNulty, A. M.; Wang, Z.; Houck, K.; et al. Increased AKT activity contributes to prostate cancer progression by dramatically accelerating prostate tumor growth and diminishing p27Kip1 expression. *J. Biol. Chem.* 2000, *275*, 24500–24505.
(11) Page, C.; Huang, M.; Jin, X.; Cho, K.; Lilja, J.; Reynolds, R. K.; Lin, J. Elevated phosphorylation of AKT and Stat3 in prostate, breast, and cervical cancer cells. *Int. J. Oncol.* 2000, *17*, 23–28.
(12) Kim, S. H.; Forman, A. P.; Mathews, M. B.; Gunnery, S. Human breast cancer cells contain elevated levels and activity of the protein kinase, PKR. *Oncogene* 2000, *19*, 3086–3094.
(13) Price, D. T.; Rocca, G. D.; Guo, C.; Ballo, M. S.; Schwinn, D. A.; Luttrell, L. M. Activation of extracellular signal-regulated kinase in human prostate cancer. *J. Urol.* 1999, *162*, 1537–1542.
(14) Nemoto, T.; Ohashi, K.; Akashi, T.; Johnson, J. D.; Hirokawa, K. Overexpression of protein tyrosine kinases in human esophageal cancer. *Pathobiology* 1997, *65*, 195–203.
(15) Shimizu, T.; Usuda, N.; Sugenoya, A.; Masuda, H.; Hagiwara, M.; Hidaka, H. Immunohistochemical evidence for the overexpression of protein kinase C in proliferative diseases of human thyroid. *Cell. Mol. Biol.* 1991, *37*, 813–821.
(16) Katayama, Y.; Sonoda, T.; Maeda, M. A Polymer Micelle Responding to the Protein Kinase A Signal. *Macromolecules* 2001, *34*, 8569–8573.
(17) Katayama, Y.; Fujii, K.; Ito, E.; Sakakihara, S.; Sonoda, T.; Murata, M.; Maeda, M. Intracellular Signal-Responsive Artificial Gene

Regulation for Novel Gene Delivery. *Biomacromolecules* 2002, *3*, 905−909.
(18) Sakakihara, S.; Fujii, K.; Katayama, Y.; Maeda, M. A novel regulation system of gene expression responding to protease signal. *Nucleic Acids Res.* 2001, Suppl. 1, 149−150.
(19) Cohen, G. M. Caspases: the executioners of apoptosis. *Biochem. J.* 1997, *326*, 1−16.
(20) Lindgren, M.; Hällbrink, M.; Prochiantz, A.; Langel, Ü. Cell-penetrating peptides. *Trends Pharmacol. Sci.* 2000, *21*, 99−103.
(21) Schwarze, S. R.; Hruska, K. A.; Dowdy, S. F. Protein transduction: unrestricted delivery into all cells? *Trends Cell Biol.* 2000, *10*, 290−295.
(22) Kaneda, Y.; Nakajima, T.; Nishikawa, T.; Yamamoto, S.; Ikegami, H.; Suzuki, N.; Nakamura, N.; Morishita, R.; Kotani, H. Hemagglutinating virus of Japan (HVJ) envelope vector as a versatile gene delivery system. *Mol. Ther.* 2003, *6*, 219−226.

BM0493887

Available online at www.sciencedirect.com
SCIENCE DIRECT®
Bioorganic & Medicinal Chemistry Letters
ELSEVIER
Bioorganic & Medicinal Chemistry Letters 14 (2004) 2787–2790

In vivo MR detection of vascular endothelial injury using a new class of MRI contrast agent

Tatsuhiro Yamamoto,[a] Kenjiro Ikuta,[a] Keiji Oi,[b] Kohtaro Abe,[b] Toyokazu Uwatoku,[b] Fuminori Hyodo,[c] Masaharu Murata,[a] Noboru Shigetani,[d] Kengo Yoshimitsu,[e] Hiroaki Shimokawa,[b] Hideo Utsumi[c] and Yoshiki Katayama[a,*]

[a]*Department of Applied Chemistry, Faculty of Engineering, Kyushu University, Fukuoka 812-8581, Japan*
[b]*Department of Cardiovascular Medicine, Kyushu University Graduate School of Medical Sciences, Fukuoka 812-8582, Japan*
[c]*Laboratory of Bio-function Science, Graduate School of Pharmaceutical Sciences, Kyushu University, Fukuoka 812-8582, Japan*
[d]*Department of Radiology, Kyushu University Hospital, Fukuoka 812-8582, Japan*
[e]*Department of Clinical Radiology, Graduate School of Medical Sciences, Kyushu University, Fukuoka 812-8582, Japan*

Received 28 February 2004; revised 19 March 2004; accepted 22 March 2004

Abstract—A new class of dye-based MRI contrast agents, EB-DTPA-Gd, was designed and synthesized. The contrast agent was found to accumulate at the site of endothelial injury when the reagent was applied to isolated porcine blood vessels or in an ex vivo experiment using rat. In vivo MR detection of vascular endothelial injury was also successful in rat with its common carotid artery injured by balloon treatment. These results indicate that EB-DTPA-Gd is potentially useful for the diagnosis of vascular diseases.

1. Introduction

Magnetic resonance imaging (MRI) has been used as an effective noninvasive diagnostic tool. For more effective diagnosis, various MRI contrast agents have been reported.[1,2] In T1-weighted MR imaging, gadolinium ion-chelate complexes have primarily been applied, as the gadolinium ion interacts with hydrogen in water molecules and enhances the T1-relaxation.[2] As a result, clearer images can be obtained when using these gadolinium ion complexes. In this context, many kinds of site-specific MR-contrast agents have been developed.[3–6] These agents have been designed with the intent of conjugating the targeting unit with the MR detection unit. In the site-specific MRI strategy, blood vessel is one of the most promising targets, as diagnosis of vascular disease in its early stages is essential to a successful treatment intervention. However, the development of such vascular disease-specific MRI has not yet been achieved. Various biomolecules such as antibodies for integrin,[3,4] ICAM-1,[5] or fibrin[6] that interact with proteins related to vascular disease have been used in the design of such MRI reagents. The use of these biomolecules, however, has proved to be impractical in terms of cost and volume of the agents. Another possible approach involves the use of synthesized organic molecules. It has been found that MS-325 (4,4-diphenylcyclohexyl phosphodiester Gd-DTPA derivative) forms a high-molecular weight complex with albumin before its adsorption onto plaque. As such, this molecule has been applied to the imaging of blood vessels in the SLE mouse.[7]

We, however, have focused our attention on endothelium lesions as a target of the MRI contrast agent for the diagnosis of vascular disease. The vascular endothelium plays an important role in the regulation of vascular homeostasis. As such, any damage to the endothelium often leads to a serious vascular disorder such as spasms in myocardial infarction.[8] In these lesional sites, it may be possible that a certain type of molecule could interact with the extracellular matrix or the smooth muscle layer through hydrophobic or electrostatic interactions due to a loss or weakening of endothelial regulation of substances.[9] We therefore

Keywords: MRI; MRI contrast agent; Cardiovascular disease; Vascular endothelial injury.
* Corresponding author. Tel.: +81-0926424206; fax: +81-0926423606; e-mail: ykatatcm@mbox.nc.kyushu-u.ac.jp

0960-894X/$ - see front matter © 2004 Elsevier Ltd. All rights reserved.
doi:10.1016/j.bmcl.2004.03.066

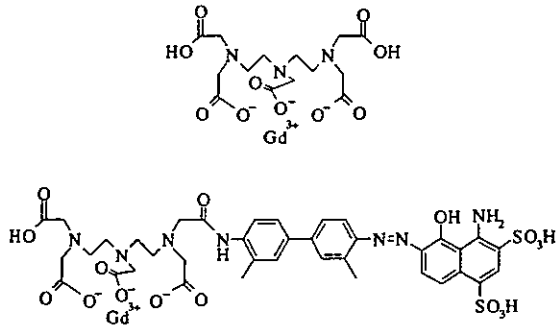

Figure 1. Chemical structure of MRI contrast agents, Gd-DTPA and EB-DTPA-Gd.

screened various organic dyes that have been used in histochemistry and found some azo-dyes that were selectively adsorbed to endothelium-denuded regions in an isolated porcine aorta sample. These dyes can interact with proteins or various tissues probably due to their good hydrophilicity or hydrophobicity balance, although accurate molecular mechanism of the binding has not been elucidated. Of these dyes, we have found Evans Blue capable of most effectively identifying the endothelium-injured region.

We have recently reported the synthesis and basic properties of an endothelium lesion-specific MRI contrast agent, EB-DTPA-Gd (Fig. 1).[10] The reagent was designed using the chemical structure of Evans Blue. This agent selectively accumulates on the endothelium-denuded surface of the porcine aorta section and enhances its signal intensity of the surface, as observed on the T1-weighted MR images.

In the present study, we applied the vascular endothelial lesion-specific contrast agent, EB-DTPA-Gd, to living rat for both ex vivo and in vivo MR imaging. First, the isolated porcine blood vessels, the endothelium of which is partially removed by scalpels, was treated with EB-DTPA-Gd in the presence of serum proteins. We next attempted ex vivo and in vivo MR imaging of the rat vascular injury at the common carotid artery, which was injured with a balloon catheter.

2. Experimental

2.1. In vitro evaluation of an isolated porcine aorta treated with EB-DTPA-Gd in the presence and absence of serum protein

A vascular endothelial lesion-specific MRI contrast agent module, EB-DTPA, was successfully synthesized, as described previously.[10,11] Complexation of EB-DTPA with gadolinium ion was achieved as follows; EB-DTPA was dissolved at 10 mM in water containing a ca. 1.5 M excess of Na_2CO_3 and equimolar gadolinium chloride was added. After adjustment to pH 7, the solution was lyophilized to obtain the desired MRI contrast agent solid, EB-DTPA-Gd. To evaluate the effects of serum proteins, EB-DTPA-Gd was dissolved in porcine serum[12] or pure water to a final concentration of 10 mM.

The specimens of porcine aorta were extracted and opened to a rectangular shape. The endothelium of the left half of the aorta was then carefully removed by scalpel (Fig. 2a). The blood vessel section was stained with each MRI contrast agent solution for 10 s and washed with saline. The aorta section was then evaluated by MR imaging (1.5 T MAGNETOM VISION system (SIEMENS, Germany), T1-weighted spin-echo, TR/TE = 400/14 ms, 3 mm slice thickness, field-of-view 50 mm, and dot matrix 128*256). The obtained MRI image was analyzed using NIH Image software.

2.2. Ex vivo or in vivo evaluation of EB-DTPA-Gd using the rat

A solid EB-DTPA-Gd was dissolved in saline to a final concentration of 24 mM. Rats (about 300 g) were anesthetized with intraperitoneal sodium pentobarbital (50 mg/kg), and then a balloon injury of the left carotid artery was made as previously described.[13] The MRI contrast agent solution was injected to the rat via the jugular vein at 160 μmol/kg. In the ex vivo experiment, the right and left common carotid arteries were extracted after 10, 30, or 120 min of reagent injection. The arteries were then opened and fixed on glass plate, and evaluated T1-weighted MR images using the same parameters as those for the in vitro experiment as described earlier.

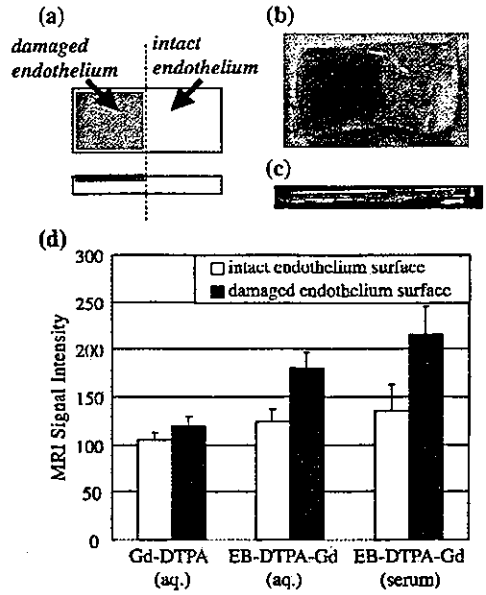

Figure 2. (a) Schematic illustration of the porcine aorta section. The left-half endothelium was removed, and the right half was intact. (b and c) The photograph and T1-weighted MR image (side view) of porcine aorta section stained with EB-DTPA-Gd in the presence of serum proteins. (d) Comparison of the surface MRI signal intensities of the porcine aorta section. The error bars represent the standard deviation ($N = 3$).

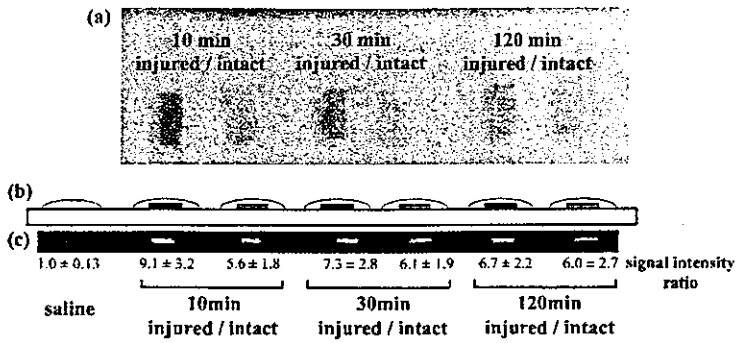

Figure 3. Ex vivo results for the opened common carotid arteries of the rat after the EB-DTPA-Gd injection via jugular vein. (a) Photograph of the extracted rat common carotid arteries at the elapsed times (10–120 min) after the injection of EB-DTPA-Gd. (b and c) Schematic illustration and MR image of both arteries dipped into saline (7 μL). The signal intensity ratio was calculated by comparing the MRI signal intensities of each artery in the saline drop with that of the saline drop alone.

The similar procedures were repeated for in vivo MR imaging of another rat. The animal was anesthetized and kept alive after its left carotid artery being injured by balloon catheter method as described.[13] After the injection of the MRI contrast agents, serial T1-weighted spin-echo MR images of the left carotid artery through transaxial plane were obtained. MR equipment used for this in vivo experiment was a 0.2 T unit (MRP-20, Hitachi, Japan). The parameters for the sequence were as follows; TR/TE = 500/25 m s, 2.5 mm slice thickness, field-of-view 200 mm, and dot matrix 256*192. As a control, 24 mM Gd-DTPA saline solution was used in a similar manner.

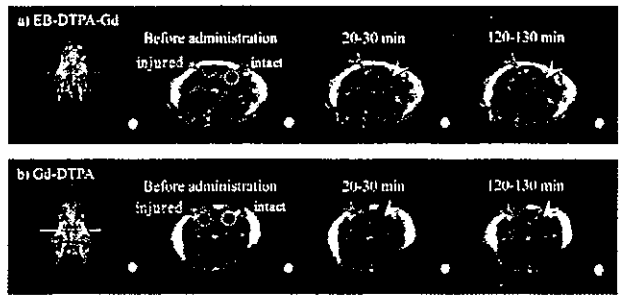

Figure 4. In vivo MR images of the rat with administration of (a) EB-DTPA-Gd and (b) Gd-DTPA via left femoral vein. The left common carotid artery was injured, and the right one was intact. The arrows in the figure indicate each artery.

3. Results and discussion

Various dyes, including Evans Blue and Congo Red, have been reported to bind to serum proteins.[14] It therefore seemed likely that EB-DTPA-Gd would also bind to serum proteins. We therefore investigated whether the presence of the serum proteins affect the characteristics of EB-DTPA-Gd, namely ability to accumulate at the sites of endothelial injury. The endothelium condition is schematically illustrated in Figure 2a. In the presence of serum proteins, EB-DTPA-Gd selectively accumulated on the endothelium injured surface (Fig. 2b). T1-weighted MR images revealed significant signal enhancement only on the endothelium-removed surface of the specimens, treated both with porcine serum and pure water solution of EB-DTPA-Gd (Fig. 2c and d). This result indicates that the serum does not affect the endothelium lesion-specific binding of EB-DTPA-Gd. The nonspecific binding of EB-DTPA-Gd slightly increased if compared with the result in the absence of serum proteins. This increase may be due to formation of the high-molecular weight complex of EB-DTPA-Gd with serum proteins.

For the next experiment, ex vivo MR imaging of the vascular endothelium injury was performed. In ex vivo study, carotid arteries with and without endothelial injury were clearly distinguished by the presence and absence of EB-DTPA-Gd accumulation, respectively, both by macroscopic observation and by T1-weighted MR images as well (Fig. 3). Figure 3c shows the MR image of the same section of aorta. The MRI signal intensity of the extracted left common carotid artery was largest after 10 min of the EB-DTPA-Gd injection. As time elapsed, the signal intensity of the left carotid artery gradually decreased, and 120 min after injection of EB-DTPA-Gd, it was almost the same as that of the right (intact side) carotid artery. The signal intensity of the right carotid artery slightly increased after EB-DTPA-Gd injection as compared to the baseline level, probably due to nonspecific binding of the contrast agent to the intact endothelium. As a site-specific contrast agent based on small organic molecule, MS-325 has been reported. The agent recognizes a inflammation site in blood vessels of SLE mice.[7] However the mechanism of the specific accumulation at the target site totally depends on the property of albumin, because the agent is carried by albumin. On the other hand, our compound possesses the recognition ability of the endothelial injury by itself.[10] Although the accurate mechanism of the recognition has not been clear.

For the final experiment, in vivo MR detection of the rat vascular injury was performed. The in vivo MRI results are shown in Figure 4. With the injection of EB-DTPA-Gd, the injured left common artery was clearly enhanced compared with the right intact common artery.

Gd-DTPA, however, did not enhance the MRI signal in either injured or intact artery. In contrast to the results of ex vivo study, the largest signal intensity of the endothelial injury was observed 120 min after EB-DTPA-Gd injection. We expected that the difference may be caused by the infiltration of the contrast agent into the tissue through the injured blood vessel surface.

4. Conclusion

Endothelial lesions are essential to the early-stage development of vascular diseases. We designed and synthesized a new dye-based MRI contrast agent, EB-DTPA-Gd, for the detection of such endothelium lesional sites. EB-DTPA-Gd was found to selectively bind to the target regions in extracted porcine aorta or living rat common carotid artery, even in the presence of serum or the blood stream. Finally, we preliminarily succeeded in carrying out noninvasive detection of injured blood vessel regions in living rat using an in vivo MRI technique. The contrast agent and the concept for the design using organic dye will be potentially useful in the development of a reliable diagnostic system that can detect vascular disease in its early stages.

Acknowledgements

This work was supported by a Grant-in-Aid for Scientific Research from the Ministry of Education, Culture, Sports, Science, and Technology of Japan and also from the Ministry of Health, Labour, and Welfare of Japan.

References and notes

1. Caravan, P.; Ellison, J. J.; McMurry, T. J.; Lauffer, R. B. *Chem. Rev.* **1999**, *99*, 2293.
2. Piguet, C.; Bunzli, J. C. G. *Chem. Soc. Rev.* **1999**, *28*, 347.
3. Sipkins, D. A.; Cheresh, D. A.; Kazemi, M. R.; Nevin, L. M.; Bednarski, M. D.; Li, K. C. *Nat. Med.* **1998**, *4*, 623.
4. Anderson, S. A.; Rader, R. K.; Westlin, W. F.; Null, C.; Jackson, D.; Lanza, G. M.; Wickline, S. A.; Kotyk, J. J. *Magn. Reson. Med.* **2000**, *44*, 433.
5. Sipkins, D. A.; Gijbels, K.; Tropper, F. D.; Bednarski, M.; Li, K. C.; Steinman, L. *J. Neuroimmunol.* **2000**, *104*, 1.
6. Yu, X.; Song, S. K.; Chen, J.; Scott, M. J.; Fuhrhop, R. J.; Hall, C. S.; Gaffney, P. J.; Wickline, S. A.; Lanza, G. M. *Magn. Reson. Med.* **2000**, *44*, 867.
7. Herborn, C. U.; Waldschuetz, R.; Lauenstein, T. C.; Goyen, M.; Lauffer, R. B.; Moeroey, T.; Debatin, J. F.; Ruehm, S. G. *Invest. Radiol.* **2002**, *37*, 464.
8. Ross, R. N. *Engl. J. Med.* **1999**, *340*, 115.
9. Bazzoni, G.; Martinez, E. O.; Dejana, E. *Trends Cardiovasc. Med.* **1999**, *9*, 147.
10. Yamamoto, T.; Ikuta, K.; Oi, K.; Abe, K.; Uwatoku, T.; Murata, M.; Shigetani, N.; Yoshimitsu, K.; Shimokawa, H.; Katayama, Y. *Anal. Sci.* **2004**, *20*, 5.
11. Precursor of the EB-DTPA, DMB-DTPA, was synthesized by the coupling of mono-Boc protected dimethylbenzidine and DTPA anhydride and was obtained as a TFA salt. The synthesis of EB-DTPA was performed as described below. All reactions were performed in an ice bath. DMB-DTPA·4TFA (0.53 g, 0.51 mmol) was dissolved in water (15 mL) containing HCl (1.52 mmol). Sodium nitrite (35 mg, 0.51 mmol) was then added in small portions, followed by stirring for 20 min. The diazonium salt solution was added dropwise into 15 mL of an aqueous 1-amino-8-naphthol-2,4-disulfonic acid (0.17 g, 0.51 mmol) solution containing sodium bicarbonate (0.43 g, 4.08 mmol), and then stirred for 3 h. The reaction mixture was lyophilized. The obtained solid was redissolved in water (10 mL), and the desired product was precipitated by concd hydrochloric acid. The precipitate was collected and dried under reduced pressure (0.36 g, 78%). The chemical structure was determined by ^{1}H NMR and elemental analysis.
12. Porcine serum was prepared as follows. Extracted porcine blood was centrifuged at 3000 rpm for 10 min to remove hemocyte. The concentrations of serum proteins obtained as the supernatant were determined to be 55 mg/mL (albumin: 33 mg/mL) by entrusting them to an outsourcer.
13. Uwatoku, T.; Shimokawa, H.; Abe, K.; Matsumoto, Y.; Hattori, T.; Oi, K.; Matsuda, T.; Kataoka, K.; Takeshita, A. *Circ. Res.* **2003**, *92*, e62.
14. Tsopelas, C.; Sutton, R. *J. Nucl. Med.* **2002**, *43*, 1377.

Photochemical Study of [3_3](1,3,5)Cyclophane and Emission Spectral Properties of [3_n]Cyclophanes (n = 2–6)

Rika Nogita, Kumi Matohara, Minoru Yamaji, Takuma Oda, Youichi Sakamoto, Tsutomu Kumagai, Chultack Lim, Mikio Yasutake, Tetsuro Shimo, Charles W. Jefford, and Teruo Shinmyozu

Contribution from Institute for Materials Chemistry and Engineering (IMCE) and Department of Molecular Chemistry, Graduate School of Sciences, Kyushu University, Hakozaki 6-10-1, Fukuoka 812-8581, Japan, Department of Chemistry, Gunma University, Kiryu, Gunma 376-8515, Japan, Institute for Molecular Science, Myodaiji, Okazaki 444-8585, Japan, Department of Chemistry, Graduate School of Science, Tohoku University, Sendai 980-8577, Japan, and Department of Applied Chemistry and Chemical Engineering, Faculty of Engineering, Kagoshima University, Korimoto 1-21-40, Kagoshima 890-0065, Japan, Departement de Chimie Organique Section de Chimie 30, Universite de Geneva, quai Ernest Ansermet CH-1211 Geneva 4, Switzerland

JOURNAL OF THE AMERICAN CHEMICAL SOCIETY®

Reprinted from
Volume 126, Number 42, Pages 13732–13741

J|A|C|S
ARTICLES
Published on Web 09/30/2004

Photochemical Study of [3$_3$](1,3,5)Cyclophane and Emission Spectral Properties of [3$_n$]Cyclophanes (n = 2−6)

Rika Nogita,[†,‡] Kumi Matohara,[†,‡] Minoru Yamaji,[§] Takuma Oda,[†,‡] Youichi Sakamoto,[#] Tsutomu Kumagai,[∥] Chultack Lim,[†] Mikio Yasutake,[†,‡] Tetsuro Shimo,[⊥] Charles W. Jefford,[¶] and Teruo Shinmyozu*[,†]

Contribution from Institute for Materials Chemistry and Engineering (IMCE) and Department of Molecular Chemistry, Graduate School of Sciences, Kyushu University, Hakozaki 6-10-1, Fukuoka 812-8581, Japan, Department of Chemistry, Gunma University, Kiryu, Gunma 376-8515, Japan, Institute for Molecular Science, Myodaiji, Okazaki 444-8585, Japan, Department of Chemistry, Graduate School of Science, Tohoku University, Sendai 980-8577, Japan, and Department of Applied Chemistry and Chemical Engineering, Faculty of Engineering, Kagoshima University, Korimoto 1-21-40, Kagoshima 890-0065, Japan, Departement de Chimie Organique Section de Chimie 30, Universite de Geneva, quai Ernest Ansermet CH-1211 Geneva 4, Switzerland

Received January 16, 2003; E-mail: shinmyo@ms.ifoc.kyushu-u.ac.jp

Abstract: Thephotochemical reaction of [3$_3$](1,3,5)cyclophane **2**, which is a photoprecursor for the formation of propella[3$_3$]prismane **18**, was studied using a sterilizing lamp (254 nm). Upon photolysis in dry and wet CH_2Cl_2 or MeOH in the presence of 2 mol/L aqueous HCl solution, the cyclophane **2** afforded novel cage compounds comprised of new skeletons, tetracyclo[6.3.1.0.^{2,7}0^{4,11}]dodeca-5,9-diene **43**, hexacyclo-[6.4.0.0.^{2,6}0.^{4,11}0.^{5,10}0^{9,12}]dodecane **44**, and pentacyclo[6.4.0.0.^{2,6}0.^{4,11}0^{5,10}]dodecane **45**. All of these products were confirmed by the X-ray structural analyses. A possible mechanism for the formation of these photoproducts via the hexaprismane derivative **18** is proposed. The photophysical properties in the excited state of the [3$_n$]cyclophanes ([3$_n$]CP, n = 2−6) were investigated by measuring the emission spectra and determining the quantum yields and lifetimes of the fluorescence. All [3$_n$]CPs show excimeric fluorescence without a monomeric one. The lifetime of the excimer fluorescence becomes gradually longer with the increasing number of the trimethylene bridges. The [3$_n$]CPs also shows excimeric phosphorescence spectra without vibrational structures for n = 2, 4, and 5, while phosphorescence is absent for n = 3 and 6. With an increase in symmetry of the benzene skeleton in the [3$_3$]- and [3$_6$]CPs, the probability of the radiation (phosphorescence) process from the lowest triplet state may drastically decrease.

1. Introduction

All members of the [3$_n$]cyclophanes ([3$_n$]CPs, n = 2−6) are available today[2,3] because of our efforts aimed at the synthesis of [3$_6$](1,2,3,4,5,6)CP **6**, [3]superphane, with bridges longer, by one carbon unit, than that of [2$_6$](1,2,3,4,5,6)CP (superphane) **7** by Boekelheide et al.[4] and Hopf et al. (Figure 1).[5] Elongation of the bridge causes the cyclophane structure to be increasingly strain-free and more flexible compared with the corresponding [2$_n$]CP series. As a result, the [3$_n$]CPs show much stronger

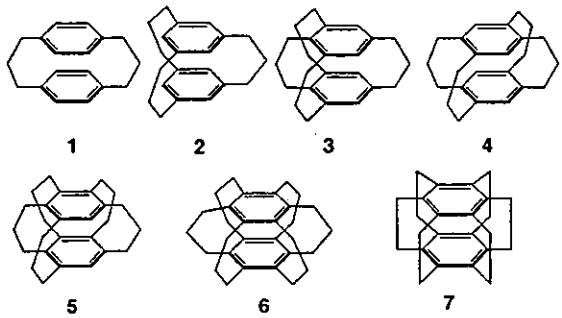

Figure 1. [3$_n$]Cyclophanes (n = 2−6) **1**−**6** and superphane **7**.

[†] Institute for Materials Chemistry and Engineering (IMCE), Kyushu University.
[‡] Department of Molecular Chemistry, Graduate School of Sciences, Kyushu University.
[§] Department of Chemistry, Gunma University.
[#] Institute for Molecular Science.
[∥] Department of Chemistry, Graduate School of Science, Tohoku University.
[⊥] Department of Applied Chemistry and Chemical Engineering, Faculty of Engineering, Kagoshima University.
[¶] Department de Chimie Organique Section de Chimie 30, Universite de Geneva.

(1) Multibridged [3n]cyclophanes, part 17.

(2) (a) Sakamoto, Y.; Miyoshi, N.; Shinmyozu, T. *Angew. Chem., Int. Ed. Engl.* **1996**, *35*, 549−550. (b) Sakamoto, Y.; Miyoshi, N.; Hirakida, M.; Kusumoto, S.; Kawase, H.; Rudzinski, J. M.; Shinmyozu, T. *J. Am. Chem. Soc.* **1996**, *118*, 12267−12275. (c) Sakamoto, Y.; Shinmyozu, T. *Recent Res. Dev. Pure Appl. Chem.* **1998**, *2*, 371−399.

(3) (a) Meno, T.; Sako, K.; Suenaga, M.; Mouri. M.; Shinmyozu, T.; Inazu, T.; Takemura, H.: *Can. J. Chem.* **1990**, *68*. 440−445. (b) Shinmyozu, T.; Hirakida, M.; Kusumoto, S.; Tomonou, M.; Inazu, T.; Rudzinski, J. M. *Chem. Lett.* **1994**, 669−672. (c) Sentou, W.; Satou, T.; Yasutake, M.; Lim, C.; Sakamoto, Y.; Itoh, T.; Shinmyozu, T. *Eur. J. Org. Chem.* **1999**, 1223−1231.

(4) (a) Sekine, Y.; Brown, M.; Boekelheide, V. *J. Am. Chem. Soc.* **1979**, *101*, 3126−3127. (b) Sekine, Y.; Boekelheide, V. *J. Am. Chem. Soc.* **1981**, *103*, 1777−1785.

10.1021/ja030032x CCC: $27.50

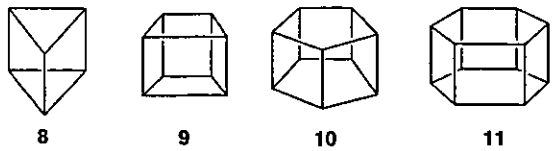

Figure 2. Prismane family.

π-electron donating ability than the corresponding [2$_n$]CPs.[2,6] We have already reported the synthetic methods of the [3$_n$]CPs and their structural properties in solution[2] as well as in the solid state.[6] Our next subject to be solved in this field is the synthesis of propella[3$_n$]prismanes via photochemical reaction of the [3$_n$]-CPs.[7,8]

Prismanes constitute an infinite family of $(CH)_n$ polyhedra[9] that chemists find esthetically appealing because of their molecular architecture (Figure 2). Notwithstanding their structural regularity, many years of effort were needed before the first three members, prismane **8**,[10] cubane **9**,[11] and pentaprismane **10**,[12] could be successfully synthesized. Recently, attention has been focused on the challenging objective of constructing the higher prismanes, in particular, hexaprismane **11**. Many diverse synthetic strategies have been developed, and significant progress toward the synthesis of hexaprismane **11** has been made.[13-16] For example, synthesized secohexaprismane, in which only one C−C bond is missing from hexaprismane **11**.[15] However, **11** has eluded synthesis so far.

Pentacyclo[6.4.0.0.^{2,7}0.^{3,12}0^{6,9}]dodeca-4,10-diene **12**, an attractive and logical precursor, could not be photochemically converted to **11** (Scheme 1).[17] This result might have been anticipated because the related olefin, *syn*-tricyclo[4.2.0.0^{2,5}]octa-3,7-diene **13** failed to give cubane **9** via [2+2]photocyclization.[18] However, the photochemical formation of propella[3$_4$]prismane **15** from diene **14** is indicative that attaching trimethylene bridges

Scheme 1. Intramolecular [2+2] Photochemical Reactions

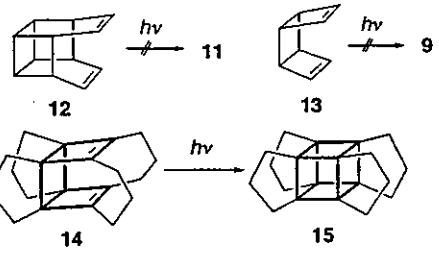

Scheme 2. Expected Photochamical Reactions

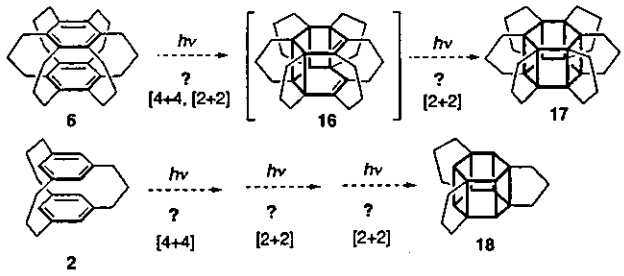

to the basic skeleton may enable [2+2]photocyclization leading to the prismane skeletons (Scheme 1).[19] These findings have been rationalized in terms of the order of the frontier molecular orbitals which are largely affected by through-bond interactions.[20-23] Moreover, on the basis of Frontier MO consideration, it was predicted that [3]superphane **6** would give the hexaprismane derivative **17** on irradiation.[20] It could be argued that three trimethylene bridges would be just as effective as six making the [3$_3$]CP **2** a likely candidate for conversion to the triply bridged hexaprismane **18** (Scheme 2). Before putting this prediction to the test, we decided to first investigate the photochemical behavior of less substituted **2** with the aim of optimizing the reaction conditions. We now describe experiments with **2**,[3a,24] the lower homologue of **6**, which has the advantage of being available in large quantities.

Benzene is very stable to photochemical reaction so that the photodimer of benzene has hardly been characterized except for a few examples, whereas the photodimer of condensed aromatics such as naphthalene and anthracene has been reported.[25] Misumi et al. first reported the novel photodimerization of benzene rings incorporated into *syn*-quadruple-layered dihetera-cyclophane **19** and concluded that the photodimerization is affected by the face-to-face stacking of two fairly strained benzene rings, as well as the substituted positions of four bridges at the inner benzenes and that the outer benzene rings are required for an increase in thermal stability of the photoisomers **20** but not for photodimerization (Scheme 3).[26] Prinzbach et al. reported a second example of the photodimerization of benzene rings in a rigid polycyclic cage, the [6+6] photocyclization between two benzene rings in solution (**21** to **22**).[27] They

(5) El-tamany, S.; Hopf, H.; *Chem. Ber.* **1983**, *116*, 1682−1685.
(6) (a) Yasutake, M.; Koga, T.; Sakamoto, Y.; Komatsu, S.; Zhou, M.; Sako, K.; Tatemitsu, H.; Onaka, S.; Aso, Y.; Inoue, S.; Shinmyozu, T. *J. Am. Chem. Soc.* **2002**, 10136−10145. (b) Yasutake, M.; Araki, M.; Zhou, M.; Nogita, R.; Shinmyozu, T. *Eur. J. Org. Chem.* **2003**, 1343−1351. (c) Yasutake, M.; Koga, T.; Lim, C.; Zhou, M.; Matsuda-Sentou, W.; Satou, T.; Shinmyozu, T. In *Cyclophane Chemistry for the 21st Century*; Takemura, H., Ed.; Research Signpost: Kerana, India, 2002, pp 265−300.
(7) (a) Sakamoto, Y.; Kumagai, T.; Matohara, K.; Lim, C.; Shinmyozu, T. *Tetrahedron Lett.* **1999**, *40*, 919−922. (b) Matohara, K.; Lim, C.; Yasutake, M.; Nogita, R.; Koga, T.; Sakamoto, Y.; Shinmyozu, T. *Tetrahedron Lett.* **2000**, *41*, 6803−6807.
(8) (a) Lim, C.; Yasutake, M.; Shinmyozu, T. *Angew. Chem., Int. Ed. Engl.* **2000**, *39*, 578−580. (b) Lim, C.; Yasutake, M.; Shinmyozu, T. *Tetrahedron Lett.* **1999**, *40*, 6781−6784.
(9) For recent reviews, see. (a) Shinmyozu, T.; Nogita, R.; Akita, M.; Lim, C. In *CRC Handbook of Organic Photochemistry and Photobiology*, 2nd edition; Horspool, W., Lench, F., Eds.; CRC Press: USA, **2003**, 23−1−23−11. (b) Dodziuk, H. In *Topics in Stereochemistry*; Eliel, E. L., Wilen, S. H., Eds.; John Wiley & Sons: New York, 1994; Vol. 21. (c) Dodziuk, H. Modern Conformational Analysis, VCH Publishers: **1995**. (d) Forman, M. A. *Org. Prep. Proced. Int.* **1994**, *26*, 291−320.
(10) Katz, T. J.; Acton, N. *J. Am. Chem. Soc.* **1973**, *86*, 2035−2037.
(11) (a) Eaton, P. E.; Cole, Jr. T. W. *J. Am. Chem. Soc.* **1964**, *86*, 962−963. (b) Eaton, P. E.; Cole, Jr. T. W. *J. Am. Chem. Soc.* **1964**, *86*, 3157−3158. (c) Eaton, P. E. *Angew. Chem., Int. Ed. Engl.* **1992**, *31*, 1421−1436.
(12) (a) Eaton, P. E.; Or, Y. S.; Branca, S. J. *J. Am. Chem. Soc.* **1981**, *103*, 2134−2136. (b) Eaton, P. E.; Or, Y. S.; Branca, S. J.; Ravi Shanker, B. K. *Tetrahedron* **1986**, *42*, 1621−1631.
(13) Eaton, P. E.; Chakraborty, U. R. *J. Am. Chem. Soc.* **1978**, *100*, 3634−3635.
(14) (a)Mehta, G.; Padma, S. *J. Am. Chem. Soc.* **1987**, *109*, 7230−7237. (b) Mehta, G.; Padma, S. *Tetrahedron* **1991**, *47*, 7807−7820.
(15) (a) Mehta, G.; Padma, S. *J. Am. Chem. Soc.* **1987**, *109*, 2212−2213. (b) Mehta, G.; Padma, S. *Tetrahedron Lett.* **1991**, *47*, 7783−7806.
(16) (a) Dailey, W. P.; Golobish, T. D. *Tetrahedron* **1996**, *37*, 3239−3242. (b) Chou, T −C.; Lin, G.-H.; Yeh, Y.-L.; Lin, K.-J. *J. Chinese Chem. Soc.* **1997**, *44*, 477−493.
(17) Yang, N. C.; Horner, M. G. *Tetrahedron Lett.* **1986**, *27*, 543−546.
(18) Iwamura, H.; Morino, K.; Kihara, H. *Chem. Lett.* **1973**, 457−460.
(19) (a) Gleiter, R.; Karcher, M. *Angew. Chem. Int. Ed. Engl.* **1988**, *27*, 840−841. (b) Brand, S.; Gleiter, R. *Tetrahedron Lett.* **1997**, *38*, 2939−2942. (c) Gleiter, R.; Brand, S. *Chem. Eur. J.* **1998**, *4*, 2532−2538.
(20) Cha, O. J.; Osawa, E.; Park, S. *J. Mol. Struct.* **1993**, *300*, 73−81.
(21) Dailey, W. P. *Tetrahedron Lett.* **1987**, *28*, 5787−5990.
(22) Disch, R. L.; Schulman, J. M. *J. Am. Chem. Soc.* **1988**, *110*, 2102−2105.
(23) Engelke R. *J. Am. Chem. Soc.* **1986**, *108*, 5799−5803 and references therein.
(24) Hubert, A. J. *J. Chem. Soc. C* **1967**, 6−10.
(25) Chandross, E. A.; Dempster, C. J. *J. Am. Chem. Soc.* **1970**, 704−706.
(26) (a) Higuchi, H.; Takatsu, K.; Otsubo, T.; Sakata, Y.; Misumi, S. *Tetrahedron Lett.* **1982**, *23*, 671−672. (b) Higuchi, H.; Kobayashi, E.; Sakata, Y.; Misumi, S. *Tetrahedron* **1986**, 42, 1731−1739.

Scheme 3. Novel Photodimerizations of Benzene Rings in the *Syn*-Quadruple-Layered Diheteracyclophane 19 and 21

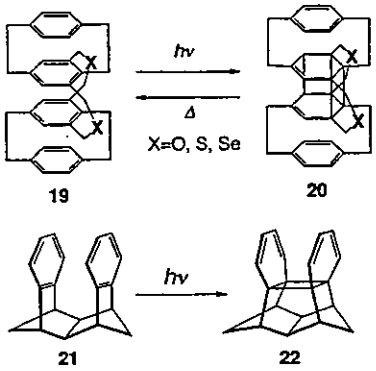

proposed a synthetic route of the doubly birdcage-annelated hexaprismane derivatives via the [2+2] photocyclization.[28] Thus, a limited number of this type [2+2] photocyclization between two benzene rings has been reported so far. In our photochemical approach to the construction of propella[3_n]prismanes, the [3_n]-CPs (n = 3−6), in which two benzene rings are completely stacked at 3.0−3.2 Å transannular distances, are used for the precursors.[6a]

The [3_n]CPs are very useful chromophores for the study of the singlet and triplet excimer states.[29] An investigation of the excimeric states of aromatic compounds in intramolecular and intermolecular systems has been reported.[25,29a] The unique spectroscopic and photochemical properties of [2.2]metacyclophane and related compounds,[30] fluorene,[31] naphthalene derivatives,[32,33] and anthracene derivatives[34] with transannular π-electronic interaction have been extensively studied as benzene dimer models.[35] Fluorescence and phosphorescence from an excimer, a transient singlet and a triplet dimer formed by the association of electronically excited and unexcited molecules, have been observed for a number of aromatic hydrocarbons in liquid solution, pure liquid, and the crystalline state. However, only in the case of benzene, observation and definite conclusion have not been drawn because of the difficulty of its measurements except for gas-phase measurement. The [3_n]CPs may elucidate this problem by behaving as a benzene dimer in the excited state due to their structural character, where the two benzene ring are completely stacked face to face by trimethylene chains. Furthermore, the [3_n]CPs should show excimer emission efficiently rather than the [2_n]CPs on the basis of a statistical rule known as Hirayama's $n = 3$ rule.[36]

Scheme 4. Bridge Flipping Process and Two Stable Conformers (C_{3h} and C_s) of [3$_3$](1,3,5)Cyclophane 2

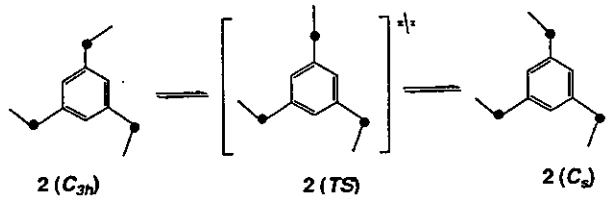

We wish to report here a photochemical study of [3$_3$]CP **2** directed toward the synthesis of the first hexaprismane derivative, propella[3$_3$]prismane **18**, and the emission spectral properties of the [3_n]CPs (n = 2−6) as fundamental information on the excited states.

2. Results and Discussion

The precursor of the photochemical reaction, [3$_3$]CP **2**, was prepared by the TosMIC coupling method as previously reported.[3a] Two conformers having C_{3h} and C_s symmetries are observed in the ^{1}H NMR spectrum of 2,2,11,11,20,20-hexadeuterated **2** in CD_2Cl_2, and **2** (C_S) is more stable than **2** (C_{3h}) by 0.4 kcal/mol. The energy barrier for the bridge flipping process is 12.4 kcal/mol (T_c = −7 °C) (Scheme 4),[3a] and the value is slightly higher than those of [3$_2$](1,3)-[37,38] and [3$_2$](1,4)-CPs.[39,40] The Density Functional calculations (B3LYP) estimated that the transition state **2** (*TS*) connecting the C_{3h} and the C_s conformers has only one flat bridge whose dihedral angle is calculated to be 180.0°, and one of three bridges can change its conformation independently without the influence of other bridges.[41] In the solid state, **2** takes the C_s conformation and the benzene rings are completely stacked with the transannular distance being 3.08−3.24 Å.[6a]

2.1. Photochemical Reaction of [3$_3$](1,3,5)Cyclophane 2. Irradiation of **2** by a sterilizing lamp (λ = 254 nm) in cyclohexane, MeOH, or benzene left **2** intact, while causing some of the usual polymerization. However, two types of products were formed when CH_2Cl_2 was used as a solvent.[7] A dry CH_2Cl_2 solution of **2** (4.90 × 10^{-3} mol/L) in a quartz vessel

(27) (a) Prinzbach, H., Sedelmeier, G.; Kruger, C.; Goddart, R.; Martin, H. D.; Gleiter, R. *Angew. Chem., Int. Ed. Eng.* **1978**, *42*, 1731−1739. (b) Fessner, W. D.; Prinzbach, H. *Tetrahedron Lett.* **1983**, *24*, 5857−5860. (c) Prinzbach, H.; Sedelmeier, G.; Krüger, C.; Goddard, R.; Martin, H. D.; Gleiter, R. *Angew. Chem. Int. Ed. Engl.* **1978**, *17*, 271−272. (d) Wollenweber, M.; Hunkler, D.; Keller, M.; Knothe, L.; Prinzbach, *Bull. Soc. Chim. Fr.* **1993**, *130*, 32−57.
(28) Wollenweber, M.; Etzkorn, M.; Reinbold, J.; Wahl, F.; Voss, T.; Melder, J. P.; Grund, C.; Pinkos, R.; Hunkler, D.; Keller, M.; Wörth, J.; Knothe, L.; Prinzbach, H., *Eur. J. Org. Chem.* **2000**, 3855−3886.
(29) (a) Lim, E. C. *Acc. Chem. Res.* **1987**, *20*, 8−17. (b) Saigusa, H.; Lim, E. C. *Acc. Chem. Res.* **1996**, *29*, 171−178.
(30) (a) Shizuka, H.; Ogiwara, T.; Morita, T. *Bull. Chem. Soc. Jpn.* **1975**, *48*, 3385−3386. (b) Ishikawa, S.; Nakamura, J.; Iwata, S.; Sumitani, M.; Nagakura, S.; Sakata, Y.; Misumi, S. *Bull. Chem. Soc. Jpn.* **1979**, *52*, 1346−1350. (c) Kovac, B.; Mohraz, M.; Heilbronner, E.; Boekelhide, V.; Hopf, H. *J. Am. Chem. Soc.* **1980**, *102*, 4314−4324. (d) Dewhirst, K. C.; Cram, D. J. *J. Am. Chem. Soc.* **1958**, 3115−3125.
(31) (a) Saigusa, H.; Itoh, M. *J. Phys. Chem.* **1985**, *89*, 5486-5488. (b) Rani, S. A.; Sobhanadri, J.; Prasada Rao, T. A. *J. Photochem. Photobio. A: Chem.* **1996**, *94*, 1−5.
(32) (a) Yamaji, M.; Tsukada, H.; Nishimura, J.; Shizuka, H.; Tobita, S., *Chem. Phys. Lett.* **2002**, *357*, 137−142. (b) Yamaji, M.; Shima, K.; Nishimura, J.; Shizuka, H.; *J. Chem. Soc., Faraday Trans. 93*, 1065−1070, **1997**.
(33) (a) Nakamura, Y.; Fujii, T.; Nishimura, J. *Tetrahedron Lett.* **2000**, *41*, 1419−1423. (b) Nakamura, Y.; Kaneko, M.; Yamanaka, N.; Tani, K.; Nishimura, J. *Tetrahedron Lett.* **1999**, *40*, 4693−4696.
(34) Kaupp, G., *Angew. Chem., Int. Ed. Engl.* **1972**, *11*, 313−314.
(35) (a) Langridge-Smith, P. R. R.; Brumbaugh, V. D.; Haynman, A. C.; Levy, H. D. *J. Phys. Chem.* **1981**, *85*, 3742−3746. (b) Hopkins. J. B.; Power, D. E.; Smalley, R. E. *J. Phys. Chem.* **1981**, *85*, 3739−3742. (b) Gonzalez, C.; Lim, E. C. *J. Phys. Chem. A* **2001**, *105*, 1904−1908.
(36) Hirayama, F.*J. Chem. Phys.* **1965**, *42*, 3163−3171.
(37) Semmelhack, M. F.; Harrison, J. J.; Young, D. C.; Gutiérrez, A.; Rafii, S.; Clardy, J. J. *J. Am. Chem. Soc.* **1985**, *107*, 7508−7514.
(38) (a) Sako, K.; Hirakawa, T.; Fujimoto, N.; Shinmyozu, T.; Inazu, T.; Horimoto, H. *Tetrahedron Lett.* **1988**, *29*, 6275−6278. (b) Sako, K.; Shinmyozu, T.; Takemura, H.; Suenaga, M.; Inazu, T. *J. Org. Chem.* **1992**, *57*, 6536−6541. (c) Shinmyozu, T.; Hirakawa. T.; Wen, G.; Osada, S.; Takemura, H.; Sako, K.; Rudzinski, J. M. *Liebigs Ann.* **1996**, 205−210. (d) Sako, K.; Tatemitsu, H.; Onaka, S.; Takemura, H.; Osada, S.; Wen, G.; Rudzinski, J. M.; Shinmyozu, T. *Liebigs Ann.* **1996**, 1645−1649. (e) Takemura. H.; Kariyazono, H.; Kon, N.; Tani, K.; Sako. K.; Shinmyozu, T.; Inazu, T. *J. Org. Chem.* **1999**, *64*, 9077−9079. (f) Wen. G.; Matsuda-Sentou, W.; Sameshima, K.; Yasutake. M.; Noda, D.; Lim. C.; Satou, T.; Takemura, H.; Sako, K.; Tatemitsu, H.; Inazu, T.; Shinmyozu, T. submitted to *J. Am. Chem. Soc.* (g) Satou, T.; Shinmyozu, T. *J. Chem. Soc., Perkin Trans. 2* **2002**, 393−397.
(39) Anet, F. A. L.; Brown, M. A. *J. Am. Chem. Soc.* **1969**, *91*, 2389−2391.
(40) Sako, K.; Meno, T.; Takemura, H.; Shinmyozu, T.; Inazu. T. *Chem. Ber.* **1990**, *123*, 639−642.
(41) Hori, K.; Sentou, W.; Shinmyozu, T. *Tetrahedron Leti.* **1997**, *38*, 8955−8958.

Scheme 5. Photochemical Reaction of [3₃](1,3,5)Cyclophane 2 in Dry CH_2Cl_2 or Wet CH_2Cl_2 (upper) and in MeOH in the Presence of 2 mol/L Aqueous HCl (lower) under Sterilizing Lamp Irradiation

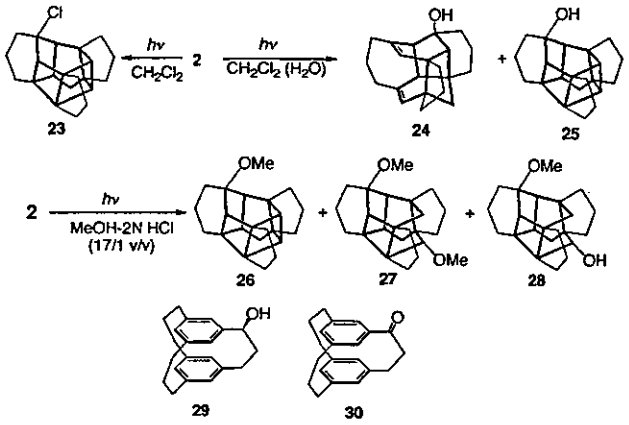

was irradiated by a sterilizing lamp for 2.5 h at room temperature under Ar. Separation of the reaction mixture by silica gel column chromatography with hexane afforded a new cage compound, the bridged hexacyclic chlorododecane **23** (5.3%) and the recovery of the starting compound **2** (40%) (Scheme 5). The structure of **23** was first proposed from the molecular formula, NMR data [the distortionless enhancement by polarization transfer (DEPT) spectrum and the ^1H-^{13}C correlation spectroscopy], elemental analysis, and mass spectral data (FABMS: m/z = 311 [$M^+ - 1$]). Furthermore, the structure was confirmed by the fact that its ^1H- and ^{13}C NMR data are quite similar to those of the alcohol **25** with the same structure as described below.[7a]

Irradiation of **2** under the same conditions as before, while in a CH_2Cl_2 solution saturated with water (1.45×10^{-2} mol/L) for 2.5 h under Ar, followed by separation by column chromatography (SiO_2, hexane:AcOEt, 10:1), gave, in addition to **2** (18%), two photoproducts. The ^1H- and ^{13}C NMR spectra of **25** are similar to those of **23**, suggesting that the two molecules have the same structure. The structure of the polycyclic olefin **24** was identified on the basis of the NMR data (^1H- and ^{13}C NMR, DEPT spectrum), elemental analysis, mass spectral data (FABMS: m/z = 294 [M^+]), and finally by X-ray structural analysis. The novel polycyclic diolefin **24** is composed of one cyclooctadiene, one cycloheptane, one cyclohexane, and two cyclohexene rings, which originate from the benzene rings, and three cyclopentanes (Figure 3A). The C3−C4 [1.340(3) Å] and C9−C10 [1.337(3) Å] bonds are double bonds. The upper and lower cyclohexenes are connected at three positions, C2−C8, C6−C7, and C5−C11 (Figure 3B). The upper cyclohexene ring takes the strained half-chair form of the cyclohexene [the dihedral angles of C2−C3−C4−C5 is −10.8(2)°]. To release this deviation, the bond lengths of C2−C8 [1.602(3) Å] and C5−C11 [1.649(3) Å] are abnormally long compared with the RHF/6-31G* optimized C−C bond length (1.552 Å) of a cyclopentane. The crystal packing diagram of **24** is shown in Figure S1 in the Supporting Information, and the crystal data of **24** as well as those of other photoproducts **25**, **27**, **28**, and **31**, which will be mentioned hereafter, are summarized in Table S1 in the Supporting Information.

The structure of the cage compound **25** was determined by X-ray structural analysis (−170 °C) (Figure 4A). Compound **25** has the highest strain energy among the identified photo-

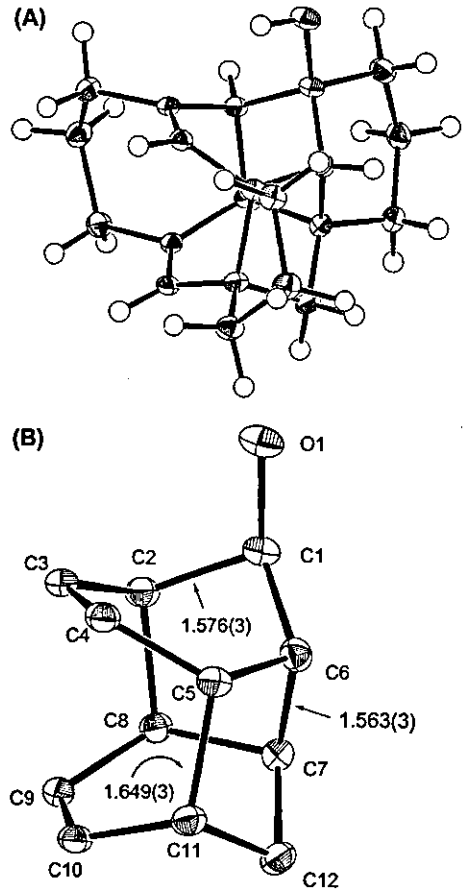

Figure 3. ORTEP drawings of the photoproduct **24** (−170 °C) (A) and its skeleton (B). Selected bond length (Å): C1−C2 1.543(3), C2−C3 1.521-(3), C3−C4 1.340(3), C4−C5 1.515 (3) C5−C6 1.563(3), C6−C1 1.538-(3), C7−C8 1.576(3), C8−C9 1.524(3), C9−C10 1.337(3), C10−C11 1.497(3), C11−C12 1.546(3), C2−C8 1.602(3), C5−C11 1.649(3), C12−C7 1.538(3).

products because it has three consecutive cyclobutane rings. The skeleton of **25** is composed of the three consecutive cyclobutane rings and two cyclopentane rings. The cyclobutane rings are not square but are rectangular, and the magnitude of the deviation is significant in the central cyclobutane ring. The C3−C12 and C4−C13 bonds are significantly longer than other C−C bonds of the cyclobutane rings. However, a detailed discussion of the C−C bond lengths cannot be provided at the present stage because of the insufficient quality of the X-ray data. A more precise X-ray analysis of **25** is in progress. The central cyclobutane ring, therefore, is expected to be more reactive than the terminal rings, and in fact, the more strained central cyclobutane ring undergoes protonation in preference to the terminal rings as described later.

To reveal the photochemical reaction mechanism, the photolysis of **2** in acidic and basic conditions was examined. A CD_3OD or CD_3CN solution of **2** (2.71×10^{-2} mol/L) containing 2 mol/L aqueous HCl solution (one drop) in a quartz NMR tube was irradiated with a sterilizing lamp for 2.5 h at room temperature under Ar, and the reaction was monitored by the ^1H NMR spectra. The reaction proceeded in acidic conditions, whereas the reaction in CD_2Cl_2 in the presence of triethylamine did not proceed. Because the reaction afforded photoproducts only in CH_2Cl_2 or CD_3CN and CD_3OD in the presence of HCl, the heavy atom effect on product formation was examined.

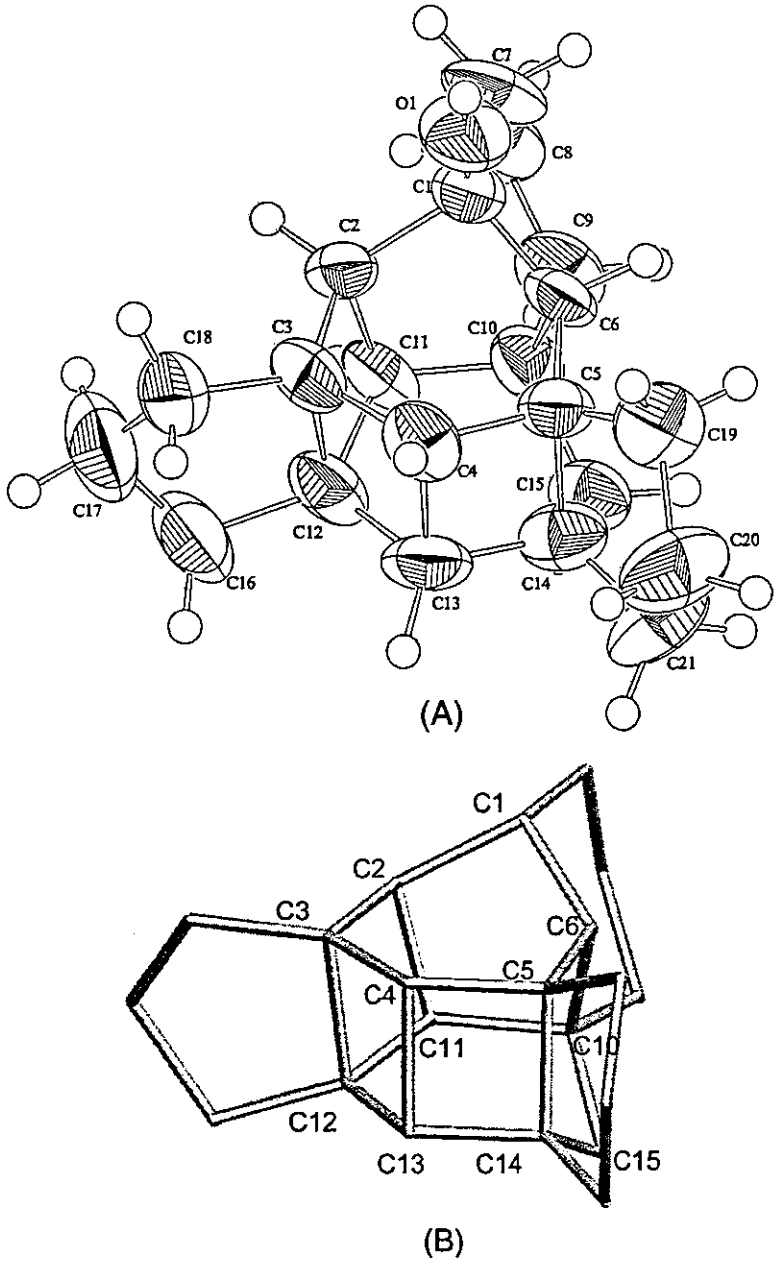

Figure 4. ORTEP drawings of the photoproduct **25** (−170 °C) (A) and its skeleton (B).

However, the reaction in CD_3OD in the presence of EtI (5 or 10 mol %) gave no photoproducts. In the preparative scale of the reaction, a mixture of MeOH and 2 mol/L aqueous HCl solution (17:1 v/v) (1.02×10^{-2} mol/L) of **2** was irradiated with a sterilizing lamp in a quartz vessel for 80 min at room temperature under Ar. Separation of the reaction mixture by recycle HPLC on GPC with $CHCl_3$ afforded the recovered **2** (11%), the methoxy compound **26** (2.7%), as well as the dimethoxy and methoxy-hydroxy compounds **27** (11%) and **28** (5.9%) with a new caged skeleton. Prolonged irradiation gave the dimethoxy compound **27** as a major product (57%). Compound **26** has the same skeleton as **23** and **25**.

In degassed nonpolar solvents such as hexane, pentane, and cyclohexane, it was found that photoreaction did not appreciably proceed. On the other hand, in the presence of dissolved oxygen in the nonpolar solvents, trace amounts of the photoproducts oxidized at the benzylic positions **29** and **30** (yield < 0.1%) were detected. The alcohol **29** was isolated from the reaction mixture and identified by the ^1H- and ^{13}C NMR (DEPT) spectra and mass spectrum. A question was raised regarding the source of this oxygen atom, oxygen gas in the solvent or singlet oxygen generated during the photoreaction. To answer this question, the reaction was conducted under the generation of singlet oxygen with 1,3-diphenyl-isobenzofuran known as a singlet oxygen monitor reagent. From this singlet oxygen reaction, the oxidized products (**29**, **30**) were obtained in a negligibly minute quantity. Therefore, it is concluded that the oxygen atom substituted at the benzylic position came from air, not from singlet oxygen.

Next, we tested the photosensitization of the [3$_3$]CP **2** (2.7×10^{-2} mol/L) containing acetone as a sensitizer (2 mg). The solution containing acetone in a Pyrex NMR tube was irradiated

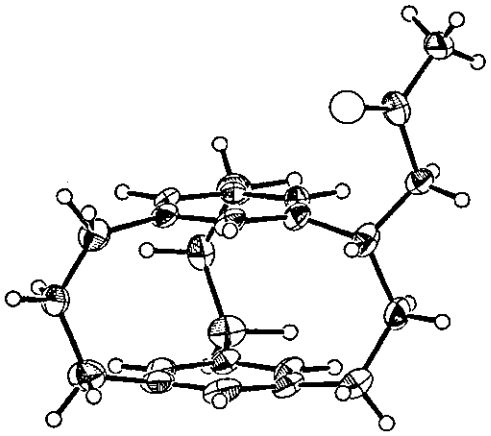

Figure 5. ORTEP drawing of 1-acetylmethyl [3₃](1,3,5)cyclophane **31** (−170 °C).

Scheme 6. Photochemical Reaction of 2 in Acetone

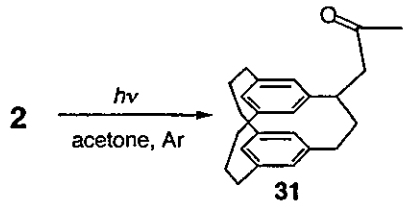

with a high-pressure Hg lamp (400 W) at room temperature under Ar, and the reaction was monitored by the ^{1}H NMR spectra. Irradiation of the benzene-d_6 solution of **2** for 26 h at room-temperature left **2** intact, whereas the irradiation of the CD_3CN solution for 26 h at room temperature caused some of the usual polymerization. However, in the photochemical reaction of the acetone-d_6 solution, products which could be monitored by the ^{1}H NMR spectrum were observed. In the preparative scale reaction, an acetone solution (3.6×10^{-3} mol/L) of **2** was irradiated with a high-pressure Hg lamp for 6 h at room temperature. Separation of the reaction mixture by silica gel column chromatography with CH_2Cl_2 afforded **31** in a small quantity (Scheme 6). It is assumed that the irradiation of **2** formed a benzyl radical intermediate caused by abstraction of a hydrogen from a benzylic methylene group, which gave **31** by the reaction with acetone. The structure of **31** was identified as 1-acetylmethyl[3₃]CP **31** by the mass spectrum, ^{1}H- and ^{13}C NMR spectra, and X-ray structural analysis (Figure 5). The role of acetone in this photochemical reaction is not clear at the present stage. The two benzene rings of **31** are completely stacked face to face similar to that of the [3₃]CP **2**, but their transannular distances are slightly longer than those of **2**. The bridged carbon−carbon distance is 3.079−3.115 Å, whereas the unbridged carbon−carbon distance is 3.124−3.175 Å.

2.2. Possible Photochemical Reaction Mechanism of [3₃]-(1,3,5)Cyclophane. There has been no conclusive evidence, but we speculated a reaction mechanism (protonation mechanism) as shown in Scheme 7. The [3₃]CP **2** on irradiation in CH_2Cl_2 first gives highly strained hexaprismane derivative **18**. However, protonation occurs at the unbridged carbon atom of a cyclobutane ring to give secondary carbocation **35**, which rearranges to the more stable tertiary carbocation **36**. Finally, **36** is intercepted by chloride or hydroxide ions to give the products **23** (X = Cl) or **25** (X = OH), respectively. One of the driving forces of a series of reactions may be the release of the steric energies. The formation of **24** can be explained by similar processes. Protonation at the unbridged cyclobutane carbon atom of the olefin **32** gives secondary carbocation **33**, which rearranges to the more stable tertiary carbocation **34**, and trapping the cation with water affords the olefin-alcohol **24**. The protons may be generated by the photolysis of CH_2Cl_2. In fact, the pH of the reaction mixture was ca. 2 after irradiation in the wet CH_2Cl_2 solution.

Scheme 7. Expected Mechanism for the Formation of the Photoproducts 24−28[a]

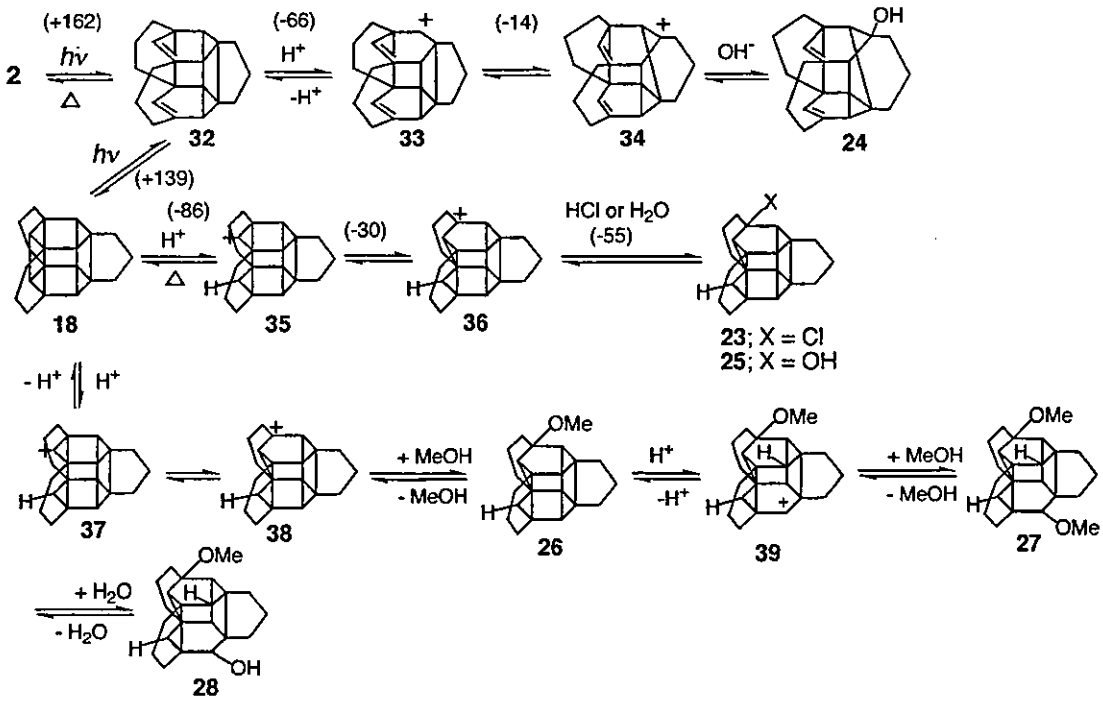

[a] The values (kcal/mol) denote the gain or release of steric energies estimated by MM3.

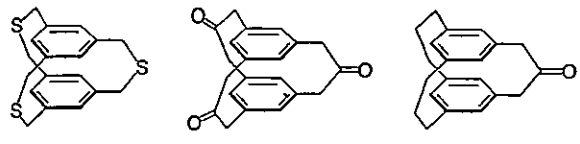

40 41 42

Figure 6. [3$_3$](1,3,5)cyclophanes **40**–**42**.

There was a possibility that **25** might be formed from **24** via [2+2] photocyclization. To examine the suggested process, a CD_2Cl_2 solution of **24** (2.38×10^{-5} mol/L) containing water (1 μL) in a quartz NMR tube was irradiated with a sterilizing lamp for 1.5 h at room temperature under Ar. The reaction was monitored by the ^{1}H NMR spectra. With a decrease in the signal intensity of **24**, the signals due to the cyclophane **2** began to appear after 30 min, and the signal intensities increased. This result suggests that the photochemical conversion between **2** and **24** is reversible. However, after 45 min, both signal intensities due to **2** and **24** were decreased, and finally the ^{1}H NMR spectrum for photoproduct(s) with no aromatic or olefinic protons appeared. Thus, the olefin **24** may convert to **25** via the cyclophane **2**. The direct conversion of **24** to **25** is unlikely, but the process via the cyclophane **2** is plausible.

The photochemical reaction of **2** did proceed in MeOH in the presence of a proton source to give **26** as was the case in CH_2Cl_2. Subsequent protonation to the unbridged carbon atom of the central bicyclo[2.2.0]hexane skeleton of **26** from the upper side may give the secondary carbocation **39**, which is intercepted by MeOH or H_2O to give the products **27** and **28**, respectively. This interception of the secondary carbocation occurred in the preferable lower side because the steric hindrance of the methoxy group and the repulsion of the lone pair on the oxygen atoms between the flag-pole bond arise if the interception occurs on the upper side. In this reaction, we were unable to isolate and characterize the highly strained propella[3$_3$]prismane **18**, a possible intermediate, because **18** may be protonated under acidic conditions. Therefore, we studied the neutral reaction conditions using a photosensitizer. An alternative single electron transfer (SET) mechanism is also considered, and the details are described in Scheme S1 in the Supporting Information. However, this mechanism is unlikely based on the experimental results.

We investigated the photochemical reaction also in the solid state with the hope of obtaining propella[3$_3$]prismane **18** because protonation of the caged photoproducts would be eliminated in the solid state. A CH_2Cl_2 solution of **2** (30 mg) in a quartz test tube was evaporated to dryness in vacuo with a rotary evaporator. The resulting thin film around the wall of the test tube was irradiated with a sterilizing lamp for 6 h at room temperature under Ar. However, no apparent change was observed in the crystal color and forms, and the ^{1}H NMR spectrum showed complete recovery of **2**. Photolysis of 2,11,20-trithia[3$_3$]CP **40**, triketone **41**, and monoketone **42** were also studied, but no reaction was observed (Figure 6).

2.3. Photophysical Properties of [3$_n$]Cyclophanes (n = 2–6). To investigate the photophysical properties of the [3$_n$]-CPs (n = 2–6), absorption and emission spectra were measured. Figure 7 shows the absorption, fluorescence and phosphorescence spectra of the [3$_n$]CPs (n = 2–6).[42] Absorption spectra were measured in degassed cyclohexane at 295 K. The absorption band at around 35 000–40 000 cm^{-1} and a much lower

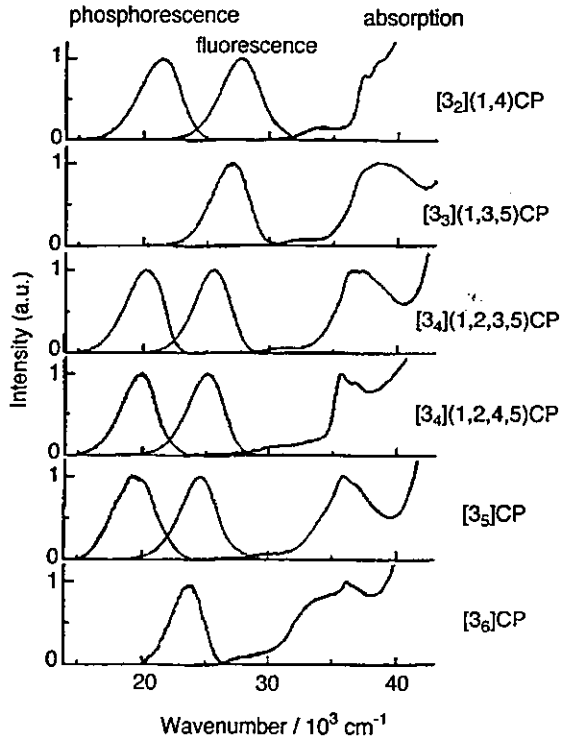

Figure 7. Absorption, fluorescence and phosphorescence spectra of [3$_n$]-cyclophanes (n = 2–6). Absorption and fluorescence spectra of the cyclophanes were obtained in degassed cyclohexane at 295 K. Phosphorescence spectra were obtained in degassed methylcyclohexane/isopentane (3:1 v/v) at 77 K.

intensity band in the region of 30 000 cm^{-1} are observed in all cyclophanes. The former band corresponding to the "cyclophane band" gradually shifts to a smaller wavenumber region with an increase in the number of trimethylene bridges. In the photochemical reaction, the excited state was generated by irradiating this band with a sterilizing lamp. The weak absorption band is due to the transannular π–π^* interaction between the two benzene rings as a benzene dimer in the ground state.[43] The appearance of this band is a characteristic phenomenon in the [3$_n$]CPs, whereas the [2$_n$]CPs (n = 2–6) and their derivatives do not show this band.

The fluorescence spectra of the [3$_n$]CPs (n = 2–6) were measured in cyclohexane at 295 K with a Hitachi F-4010 fluorescence spectrophotometer. All cyclophanes show broad fluorescence bands without vibrational structures in the region of 20 000–30 000 cm^{-1} due to the excimer interaction.[43] It was confirmed that the fluorescence excitation spectra of the [3$_n$]-CPs agreed well with the corresponding absorption spectra. The excimeric fluorescence band shifts to a smaller wavenumber with the increasing number of the trimethylene bridges. The maximum wavelengths for the absorption and emission spectra of the [3$_n$]CPs are listed in Table 1.

The quantum yield (Φ_f) of the fluorescence was determined by comparing the correct fluorescence spectrum of the [3$_n$]CP with that of mesitylene in cyclohexane, which is reported to

(42) One of the reviewers suggested that Figure 7 should report the absorption coefficients of all compounds. But the low solubility of the higher members of [3$_n$]CPs, especially [3$_6$]CP, in cyclohexane inhibited the determination of the absorption coefficients. Absorption spectra of [3$_n$]CPs in $CHCl_3$ were already reported in ref 2b.

(43) Birks, J. B. *Photophysics of Aromatic Compounds*; John Wiley & Sons: New York, 1970.

Table 1. Maximum Wavelengths of Absorption and Emission Spectra of the [3$_n$]cyclophanes (n = 2–6)

compound	λ_{max}/nm[a]	λ_{max}^{fluo}/nm[a]	λ_{max}^{phos}/nm[b]
[3$_2$]CP 1	267	360	470
[3$_3$]CP 2	258	370	
[3$_4$](1,2,3,5)CP 3	270	390	495
[3$_4$](1,2,4,5)CP 4	280	400	500
[3$_5$]CP 5	280	405	515
[3$_6$]CP 6	275	420	

[a] In cyclohexane at 295 K. [b] In a mixture of methylcyclohexane/isopentane (3:1 v/v) at 77 K.

have a Φ_f value of 0.088.[44] The rates (k_f) of the fluorescence were obtained by eq 1.

$$k_f = \Phi_f \tau_f^{-1} \quad (1)$$

The lifetimes (τ_f) of the [3$_n$]CPs were determined by time-correlated single photon counting with an Edingburg FL-900 fluorescence photometer. It is interesting that the lifetime (τ_f) becomes gradually longer with an increase in the number of trimethylene bridges. The quantum yields of the [3$_n$]CPs are considerably smaller than that of mesitylene as a reference compound. The deactivation process from the singlet state to other states via intersystem crossing or internal conversion, singlet or triplet reactions may occur much more rapidly than in mesitylene. For example, the total quantum yield of the [3$_3$]-CP 2 during the photochemical reaction was estimated to be ca. 10^{-4}.

Phosphorescence spectra were measured in methylcyclohexane-isopentane (3:1 v/v, MP) glass at 77 K using a mechanical chopper incorporated in a Hitachi F-4010 fluorescence spectrometer. The maximum wavelengths of the phosphorescence observed are listed in Table 1. With the [3$_n$]CPs for n = 2, 4, and 5, broad phosphorescence spectra without vibrational structures are seen in the region of 15 000–25 000 cm^{-1}, which are considered to originate from the triplet excimer state of the cyclophanes as a benzene dimer. On the other hand, quite interestingly, phosphorescence from [3$_3$]CP 2 and [3$_6$]CP 6 was not observed at all with the Hitachi F-4010 fluorescence spectrometer.

These observations suggest that the molecular distortion, transannular strain, and distances of the two benzene rings stacked face to face are significant factors, as was suggested by the study of the triplet excimer of naphthalenophane.[45,46] Aromatic triplet excimers play an important role and show an attractive character. Lim and co-workers reported the molecular triplet excimer of naphthalene derivatives in solution.[29] It is reported that the face-to-face stacking of two fairly strained benzene rings of the cyclophanes and a sandwich-pair or parallel conformation of the tethered chromophores are favored for singlet excimers. In contrast to the singlet excimer, a triplet excimer prefers an L-shaped arrangement.[29] In the case of the [3$_n$]CPs, two benzene rings are completely stacked with each other, but a slight conformational change has to take place in the excited state when n = 2, 4, and 5 but not for the n = 3 and 6. Table 3 shows the distances of two benzene rings of the [3$_n$]-CPs (n = 2–6) obtained by X-ray structural analyses.[6a] The transannular distances between two benzene rings of unbridged carbons (a) and bridged carbons (b), as well as the difference between them (Δ), are summarized. The benzene ring is more distorted in the [3$_n$]CPs (n = 2,[47] 4, 5) than in the [3$_n$]CPs (n = 3, 6) in the ground state. This is the reason the [3$_3$]- and [3$_6$]-CPs do not show triplet excimer phosphorescence. The order of the lifetime (τ_p) is similar to that of mesitylene, suggesting that the electronic structure of the excited triplet state is similar to that of mesitylene.

Table 2. Quantum Yields (Φ_f), Lifetimes of Fluororescence (τ_f), Rate Constants for Fluorescence (k_f) in the Degassed Cyclohexane Solution of Mesitylene and [3$_n$]cyclophanes (n = 2–6) Obtained at 295 K, and the Lifetime of Phosphorescence (τ_p) in a Mixture of Methylcyclohexane and Isopentane (3:1 v/v) at 77 K

compounds	Φ_f[a]	τ_f/ns	k_f[b]/10^5 s^{-1}	τ_p/s
mesitylene	0.088[c]	37.3	23.6	6.3
[3$_2$](1, 4)CP: 1	0.012	30.3	4.0	6.0
[3$_3$](1, 3, 5)CP: 2	0.013	31.5	4.1	[d]
[3$_4$](1, 2, 3, 5)CP: 3	0.019	62.3	3.0	1.7
[3$_4$](1, 2, 4, 5)CP: 4	0.020	67.8	3.0	3.4
[3$_5$]CP: 5	0.014	116	1.2	1.2
[3$_6$]CP: 6	0.004	160	0.25	[d]

[a] Errors ± 0.001. [b] Determined by the equation, $k_f = \Phi_f \tau_f^{-1}$. [c] Data from *J. Phys. Chem.* **1972**, *76*, 3566. [d] No detection.

Table 3. Transannular Distances of Benzene Rings of [3$_n$]cyclophanes (n = 2–6).

	a (Å)	b (Å)	Δ (a – b)
[2$_2$](1,4)CP[c])	3.09	2.78	0.31
[3$_2$](1,4) CP 1	3.30	3.14	0.16
[3$_3$](1,3,5) CP 2	3.14	3.09	0.05
[3$_4$](1,2,3,5) CP 3	3.20	2.98–3.12	0.22–0.08
[3$_4$](1,2,4,5) CP 4	3.24	3.03	0.17
[3$_5$](1,2,3,4,5) CP 5	3.24	2.93–3.07	0.31–0.17
[3$_6$](1,2,3,4,5,6) CP 6	–	2.93	–

[a] Distances of unbridged carbon atoms. [b] Distances of bridged carbon atoms: Δ (a – b) indicates the difference between a and b. [c] Data from *J. Am. Chem. Soc.* **1954**, *76*, 6132.

3. Conclusions

Irradiation of **2** with a sterilizing lamp in solutions of dry and wet CH_2Cl_2 gave prismane derivatives, the bishomopentaprismyl chloride **23**, its hydroxy analogue **25**, and the triply bridged hexacyclic dienol **24**. We speculated a protonation mechanism. Irradiation of **2** would give highly strained hexaprismane derivative **18**, which undergoes protonation of a cyclobutane ring to give a carbocation species. Interception of the carbocation gives photoproducts. This reaction proceeds in acidic conditions; photolysis of **2** in MeOH/2 mol/L aqueous HCl (17:1 v/v) with a sterilizing lamp afforded the new polycyclic caged dimethoxy and methoxy-hydroxy compounds **27** and **28** with a novel pentacyclo[6.4.0.0.^{3,7}0.^{4,11}0^{5,10}]dodecane skeleton **45**, in addition to methyl ether **26** with bishomopentaprismane **44**. Because isolation and characterization of the highly strained **18** are expected to be impossible under acidic conditions, we examined neutral reaction conditions. The reaction of **2** in

(44) Froehlich, P. M.; Morrison, H. A. *J. Phys. Chem.* **1972**, *76*, 6(24), 3566–3570.
(45) East, A. L. L.; Lim, E. C. *J. Chem. Phys.* **2000**, *113*, 8981–8994.
(46) Yamaji, M.; Tsukada, H.; Nishimura, J.; Shizuka, H.; Tobita, S. *Chem. Phys. Lett.* **2002**, *357* 137–142.
(47) (a) Gantzel, P. K.; Trueblood, K. N. *Acta Cryst.* **1965**, *18*, 958–968.

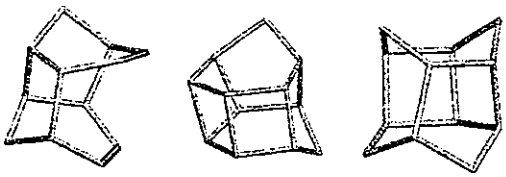

43 44 45

Figure 8. Skeletons of the new cage compounds.

acetone did not afford cage compounds except for the 1-acetylmethyl[3_3]CP **31**.

Although we have not yet succeeded in the isolation of propella[3_3]prismane **18**, we expected that **18** would be generated via the excited singlet state after irradiation of [3_2]CP **2**. Further investigations of the photochemical reaction conditions via the excited singlet state of **2**, as well as modifications of the structure of **2** in order to stabilize the hexaprismane skeleton, may lead to the isolation of the hexaprismane derivatives. The photochemical reaction of [3_6]CP **6** and fluorinated [3_3](1,3,5)-CPs are in progress, and the results will be reported soon. The photochemical reactions in the present work provide useful one-step synthetic methods leading to new polycyclic cage compounds with novel skeletons **43**−**45** from the [3_3]CP **2** (Figure 8).

All of the [3_n]CPs (n = 2−6) show excimeric fluorescence without monomer fluorescence. The lifetime gradually becomes longer with an increase in the number of the bridges. The phosphorescence from the [3_n]CPs is also observed when n = 2, 4, and 5, although it is absent for n = 3 and 6. To clarify this phenomenon in more detail, a transient absorption spectral study of the [3_n]CPs (n = 2−6) is in progress, and the results will be reported elsewhere.

4. Experimental Section

General Procedures. Melting points were measured on a Yanako MP−S3 micro melting point apparatus. ^{1}H and ^{13}C NMR spectra were measured on JEOL JNM-GX 270 and AL-300 spectrometers. Chemical shifts were reported as δ values (ppm) relative to internal tetramethylsilane (TMS) in $CDCl_3$ unless otherwise noted. Mass spectra (EIMS ionization voltage 70 eV) and fast atom bombardment mass spectra (FAB-MAS *m*-nitrobenzyl alcohol) were obtained with a JEOL JMS−SX/SX 102A mass spectrometer. Gas chromatograph mass spectrometer was measured on a SHIMADZU GCMS-QP5050A. Electronic spectra were recorded on a Hitachi U-3500 spectrometer. Infared data were obtained on a Hitachi Nicolet I-5040 FT-IR spectrometer. Elemental analyses were performed by the Service Centre of the Elemental Analysis of Organic Compound affiliated with the Faculty of Science, Kyushu University. Analytical thin-layer chromatography (TLC) was performed on Silica gel 60 F_{254} Merk and Merk Aluminumoxide 60 GF_{254} neutral (TypeE). Column chromatography was performed on Merk Silica gel 60 (40−63 μm).

All solvents and reagents were of reagent quality, purchased commercially, and used without further purification, except as noted below. Aldrich anhydrous CH_2Cl_2 (99.8%) was used for photochemical reaction. MeOH was distilled from magnesium methoxide and acetone was distilled from $CaSO_4$.

As a light source of the photochemical reactions, we used TOSHIBA-GL sterilizing lamps (10 W × 7) in place of a low-pressure Hg lamp.

Absorption and emission spectra were measured with a U-best V-550 spectrophotometer (JASCO) and a Hitachi F-4010 fluorescence spectrometer, respectively. The samples for emission measurements were degassed on a high vacuum line by freeze−pump−thaw cycles. It was confirmed that the excitation spectra of emission from the employed cyclophanes agreed well with the corresponding absorption spectra. The absolute fluorescence quantum yield was determined by comparing the corrected fluorescence spectra of cyclophanes with that of mesitylene in cyclohexane which is known to have a fluorescence quantum yield of 0.088.[44] The fluorescence lifetime was determined by single-photon counting method with a FL-900 CDT spectrophotometer (Edinburgh Analytical Instruments, UK).

X-ray Crystallographic Study. The X-ray structural analyses were obtain with a Rigaku RAXIS−IV imaging plate area detector with graphite monochromated Mo−K_α λ = 0.71070 Å) radiation and rotating anode generator. The crystal structure was solved by the direct method [SIR88][48] (**24**, **31**) [SHELXS86][49] (**25**), and [SIR92][50] (**27**, **28**), and refined by the full-matrix least-squares methods.[51] The non-hydrogen atoms were refined anisotropically, and hydrogen atoms were isotoropically. All computations were performed using the teXsan package.[52] The computations were performed with MM3(92)[53] and the Gaussian 94 program[54] graphically facilitated by Insight II from Ryoka Systems, Inc., on Silicon Graphics Octane.

Photochemical Reaction of [3_3](1,3,5)Cyclophane 2. (1) Photolysis of 2 in Dry CH_2Cl_2. A dry CH_2Cl_2 solution (650 mL) of **2** (880 mg, 3.29 mmol) in a quarz vessel was irradiated with sterilizing lamps (10 W × 7) under Ar for 150 min at room temperature. After removal of the solvent under reduced pressure, the residue was separated by SiO_2 column chromatography (hexane) to give bishomo-prismyl chloride **23** (53.1 mg, 5.2%) and the recovery of the starting **2** (352 mg, 40%). **23**: mp 68.5−70.0 °C; ^{1}H NMR δ 1.23 (d, J = 11.9 Hz, 1H), 1.47 (d, J = 11.9 Hz, 1H), 1.41−1.73 (m, 11H), 1.64 (s, 1H), 1.82−2.09 (m, 7H), 2.07 (s, 2H), 2.14 (d, J = 6.3 Hz, 1H), 2.40 (d, J = 6.3 Hz, 1H); ^{13}C NMR (DEPT) δ 21.2 (sec.), 30.2 (sec.), 31.1 (sec.), 36.2 (sec.), 37.4 (two sec.), 38.6 (sec.), 39.7 (tert.), 40.1 (sec.), 40.7 (sec.), 42.1(sec.), 43.0 (quat.), 45.8 (quat.), 47.2 (tert.), 49.5 (tert.), 53.9 (tert.), 55.8 (quat.), 58.2 (quat.), 59.7 (quat.), 65.8 (tert.), 74.5 ppm (quat.); MS (FAB, *m/z*) 311 [M^+-H]. Anal. Calcd for $C_{21}H_{25}Cl$: C, 80.62; H, 8.05%. Found: C, 80.42; H, 8.04%.

(2) Photolysis of 2 in Wet CH_2Cl_2. A water-saturated CH_2Cl_2 solution (200 mL) of **2** (800 mg, 2.89 mmol) in a quartz vessel was irradiated with sterilizing lamps (10 W × 7) under Ar for 150 min at room temperature. After removal of the solvent under reduced pressure, the residue was separated by SiO_2 column chromatography (hexane/AcOEt, 10:1) to afford polycyclic olefinic compound **24** (144 mg, 17%, R_f = 0.30), polycyclic hydroxy dodecane **25** (47 mg, 5.4%, R_f = 0.18), and the recovery of the starting **2** (143 mg, 18%). **24**: colorless crystals (toluene), mp 115.5−119.0 °C; ^{1}H NMR δ 1.34 (t, J = 1.6 Hz, 1H), 1.18−2.05 (m, 14H), 1.43 (d, J = 2.64 Hz, 2H), 2.15−2.48 (m, 4H), 2.33 (dd, J = 7.59 Hz, 1H), 2.53 (dd, J = 7.59 Hz, 1H), 2.79 (s, 1H), 5.12 (s, 1H), 5.60 (s, 1H); ^{13}C NMR (DEPT) δ 20.3 (sec.), 26.3 (sec.) 28.2 (sec.), 33.8 (sec.), 33.9 (sec.), 34.4 (sec.), 35.4 (sec.), 35.7 (sec.),

(48) Burla, M. C.; Camalli, M.; Cascarano, G.; Giacovazzo, C.; Polidori, G.; Spagna, R.; Viterbo, D. *J. Appl. Cryst.* **1989**, *22*, 389−303.
(49) Sheldrick, G. M. In *Crystallographic Computing 3*; Sheldrick, G. M., Kruger, C., Goddard, R., Eds.; Oxford University Press: New York, 1985; 175−189.
(50) Altomare, A.; Burla, M. C.; Camalli, M.; Cascarano, M.; Giacovazzo, C.; Guagliardi, A.; Polidori, G. *J. Appl. Cryst.* **1994**, *27*, 435.
(51) Sheldrick, G. M. Program for the Solution of Crystal Structures; University of Goettingen, Germany, 1997.
(52) Crystal Structure Analysis Package, Molecular Structure Corporation (1985 and 1999).
(53) The computations were performed with MM3-92, graphically facilitated by CAChe from Fijitsu Ltd. MM3-Program obtained from Technical Utilization Corporation. The program was developed by N. L. Allinger and co-workers, University of Georgia. For ab initio MO calculations, the Gaussian 94 program,[54] graphically facilitated by Insight II from Ryoka Systems Inc. on Silicon Graphics Octane, was used.
(54) Frisch, M. J.; Trucks, G. W.; Schlegel, H. B.; Gill, P. M. W.; Johnson. B. G.; Robb, M. A.; Cheeseman, J. R.; Keith, T.; Petersson, G. A.; Montgomery, J. A.; Raghavachari, K.; Al-Laham, M. A.; Zakrzewski, V. G.; Ortiz, J. V.; Foresman, J. B.; Cioslowski, J.; Stefanov, B. B.; Nanayakkara, A.; Challacombe, M.; Peng, C. Y.; Ayala, P. Y.; Chen, W.; Wong, M. W.; Andres, J. L.; Replogle, E. S.; Gomperts, R.; Martin, R. L.; Fox, D. J.; Binkley, J. S.; Defrees, D. J.; Baker, J.; Stewart, J. P.; Head-Gordon, M.; Gonzalez, C.; Pople, J. A. Gaussian, Inc., Pittsburgh, PA, 1995.